SPANDIDOS PUBLICATIONS

ONCOLOGY LETTERS 27: 70, 2024

Prediction and verification of the prognostic biomarker *SLC2A2* and its association with immune infiltration in gastric cancer

WEIJIAN ZHANG[1,2*], DISHU ZHOU[2*], SHUYA SONG[2], XINXIN HONG[3], YIFEI XU[3], YUQI WU[1], SHITING LI[1], SIHUI ZENG[1], YANZI HUANG[3], XINBO CHEN[3], YIZHONG LIANG[3], SHAOJU GUO[3], HUAFENG PAN[2] and HAIWEN LI[3]

[1]The Fourth Clinical Medical College, Guangzhou University of Chinese Medicine, Shenzhen, Guangdong 518033; [2]Science and Technology Innovation Center, Guangzhou University of Chinese Medicine, Guangzhou, Guangdong 510006; [3]Department of Gastroenterology, Shenzhen Traditional Chinese Medicine Hospital, The Fourth Clinical Medical College of Guangzhou University of Chinese Medicine, Shenzhen, Guangdong 518033, P.R. China

Received July 1, 2023; Accepted November 15, 2023

DOI: 10.3892/ol.2023.14203

Abstract. Gastric cancer (GC) is the fifth most common cause of cancer-associated deaths; however, its treatment options are limited. Despite clinical improvements, chemotherapy resistance and metastasis are major challenges in improving the prognosis and quality of life of patients with GC. Therefore, effective prognostic biomarkers and targets associated with immunological interventions need to be identified. Solute carrier family 2 member 2 (*SLC2A2*) may serve a role in tumor development and invasion. The present study aimed to evaluate *SLC2A2* as a prospective prognostic marker and chemotherapeutic target for GC. *SLC2A2* expression in several types of cancer and GC was analyzed using online databases, and the effects of *SLC2A2* expression on survival prognosis in GC were investigated. Clinicopathological parameters were examined to explore the association between *SLC2A2* expression and overall survival (OS). Associations between *SLC2A2* expression and immune infiltration, immune checkpoints and IC_{50} were estimated using quantification of the tumor immune contexture from human RNA-seq data, the Tumor Immune Estimation Resource 2.0 database and the Genomics of Drug Sensitivity in Cancer database. Differential *SLC2A2* expression and the predictive value were validated using the Human Protein Atlas, Gene Expression Omnibus, immunohistochemistry and reverse transcription-quantitative PCR. *SLC2A2* expression was downregulated in most types of tumor but upregulated in GC. Functional enrichment analysis revealed an association between *SLC2A2* expression and lipid metabolism and the tumor immune microenvironment. According to Gene Ontology term functional enrichment analysis, *SLC2A2*-related differentially expressed genes were enriched predominantly in 'chylomicron assembly', 'plasma lipoprotein particle assembly', 'high-density lipoprotein particle', 'chylomicron', 'triglyceride-rich plasma lipoprotein particle', 'very-low-density lipoprotein particle'. 'intermembrane lipid transfer activity', 'lipoprotein particle receptor binding', 'cholesterol transporter activity' and 'intermembrane cholesterol transfer activity'. In addition, 'cholesterol metabolism', and 'fat digestion and absorption' were significantly enriched in the Kyoto Encyclopedia of Genes and Genomes pathway analysis. Patients with GC with high *SLC2A2* expression had higher levels of neutrophil and M2 macrophage infiltration and a significant inverse correlation was observed between *SLC2A2* expression and MYC targets, tumor mutation burden, microsatellite instability and immune checkpoints. Furthermore,

Correspondence to: Dr Haiwen Li, Department of Gastroenterology, Shenzhen Traditional Chinese Medicine Hospital, The Fourth Clinical Medical College of Guangzhou University of Chinese Medicine, 1 Fuhua Road, Futian, Shenzhen, Guangdong 518033, P.R. China
E-mail: 370062941@qq.com

Dr Huafeng Pan, Science and Technology Innovation Center, Guangzhou University of Chinese Medicine, 232 East Outer Ring Road, Panyu, Guangzhou, Guangdong 510006, P.R. China
E-mail: gzphf@gzucm.edu.cn

[*]Contributed equally

Abbreviations: GC, gastric cancer; SLC2A2, solute carrier family 2 member 2; GLUT2, glucose transporter type 2; TMB, tumor mutation burden; TCGA, The Cancer Genome Atlas; GTEx, Genotype-Tissue Expression; DEG, differentially expressed gene; GO, Gene Ontology; KEGG, Kyoto Encyclopedia of Genes and Genomes; BP, biological process; CC, cellular component; GSEA, gene set enrichment analysis; GITR, glucocorticoid-induced tumor necrosis factor-related; TNFRSF18, TNFR superfamily 18; PDCD1, programmed cell death 1; CTLA4, cytotoxic T-lymphocyte associated protein 4; SIGLEC15, sialic acid binding Ig-like lectin 15; IHC, immunohistochemistry; SIRPα, signal regulatory protein α; DSS, disease-specific survival; PFI, progression-free interval; HPA, Human Protein Atlas; GEO, Gene Expression Omnibus; OS, overall survival; MSI, microsatellite instability; TMA, tissue microarray; HR, hazard ratio

Key words: SLC2A2, GC, prognosis, biomarker, immune infiltration

patients with high *SLC2A2* expression had worse prognosis, including OS, disease-specific survival and progression-free interval. Multivariate regression analysis demonstrated that *SLC2A2* could independently prognosticate GC and the nomogram model showed favorable performance for survival prediction. *SLC2A2* may be a prospective prognostic marker for GC. The prediction model may improve the prognosis of patients with GC in clinical practice, and *SLC2A2* may serve as a novel therapeutic target to provide immunotherapy plans for GC.

Introduction

Gastric cancer (GC) is the fifth most common cause of cancer-associated deaths worldwide, with limited treatment options (1,2). However, most patients with GC exhibit insidious onset and no obvious symptoms in the early stage, which leads to the clinical diagnosis of GC in the advanced stage (3). In 2020, >1 million new cases of stomach cancer and ~770,000 deaths from stomach cancer were reported, with about half of all new cases and related deaths occurring in China (4). According to previous studies, early detection of GC leads to favorable prognosis, whereas advanced stages of GC have worse prognoses, with survival rates of <20% (3-5). Targeted and novel immune-based therapies have become more accessible, improving the survival and prognosis of patients with GC (6,7). There is a need to identify effective immunological intervention-associated prognostic biomarkers and targets (8).

Solute carrier family 2 member 2 (*SLC2A2*), also known as glucose transporter type 2 (GLUT2), belongs to the GLUT family and is primarily responsible for transporting glucose into cells (9,10). According to previous research, tumor cells transport glucose to intracellular stores to meet their high metabolic energy demands via the SLC2A protein, suggesting that the expression of different SLC2A subtypes may be associated with invasiveness and progression of tumors (10). High *SLC2A2* expression is positively associated with a higher overall survival (OS) rate in liver and breast cancer and other malignant tumors (10,11). However, to the best of our knowledge, the association between *SLC2A2* expression and GC prognosis is unknown.

In the present study, Kaplan-Meier curves were used to investigate the association between survival prognosis and *SLC2A2* expression in GC, and the association between *SLC2A2* expression and MYC targets, tumor mutation burden (TMB), microsatellite instability (MSI), immune infiltration, immune checkpoints and IC_{50} was explored to assess the relationship between *SLC2A2* expression and immunotherapy effect. Finally, the association between SLC2A2 expression and clinical features was investigated and a predictive nomogram model was established and verified to assess the OS rate of GC. The objective of the present study was to evaluate whether *SLC2A2* could be used as a prognostic biomarker and a novel immunotherapy target for GC to improve the early diagnosis rate of GC and provide a novel regimen for immunotherapy of GC.

Materials and methods

Data collection and preprocessing. A standardized pan-cancer dataset that combined The Cancer Genome Atlas (TCGA) and Genotype-Tissue Expression (GTEx) data was downloaded from the University of California, Santa Cruz genome browser (xenabrowser.net/). Data on RNA sequencing and corresponding clinical features of stomach adenocarcinoma were obtained from TCGA (portal.gdc.cancer.gov/). All transcripts per million values were generated from fragments per kilobase million data and unified into log-transformed data (12). The present study adhered to GTEx (https://commonfund.nih.gov/GTEx) and TCGA publication guidelines (http://cancergenome.nih.gov/publications/publicationguidelines).

Differential SLC2A2 expression in cancer and GC. Using the Wilcoxon rank-sum test, *SLC2A2* expression was compared between cancer and normal tissues (healthy individuals, and adjacent tissues from the same or different patients) based on data downloaded from TCGA and GTEx. To identify differentially expressed genes (DEGs) in GC, *SLC2A2* median expression in stomach adenocarcinoma samples was used as a cut-off value to divide patients into the low and high *SLC2A2* groups. A correlation heat map was constructed to display the association between *SLC2A2* and the top 12 significant DEGs using R software (version 3.6.3; https://www.r-project.org/). DESeq2 was used to analyze data using R software (version 3.6.3; https://www.r-project.org/). An adjusted P-value (P.adj)<0.05 and |log fold-change (FC)|>2 were considered to indicate statistically significant DEGs.

Functional analysis of SLC2A2 in GC. To illustrate DEG-associated biological functions, the 'clusterProfiler' (version3.14.3;https://guangchuangyu.github.io/software/clusterProfiler) package was used for Gene Ontology (GO) and Kyoto Encyclopedia of Genes and Genomes (KEGG) enrichment analyses. Gene symbols were transformed into EntrezID to obtain GO and KEGG functional annotations using org.Hs.eg.db (version 3.12.0; https://www.bioconductor.org/packages/org.Hs.eg.db). GO enrichment analysis was divided into three categories: Biological processes (BPs), molecular functions (MFs) and cellular components (CCs). Gene set enrichment analysis (GSEA; http://www.broadinstitute.org/gsea) was conducted to examine the differential pathways and biological functions associated with *SLC2A2* expression, including GO enrichment analysis, Reactome pathway analysis and Wiki pathways analysis based on the C2 collection from the Molecular Signatures Database (https://www.gsea-msigdb.org/gsea/msigdb). A false discovery rate q-value <0.25 and P.adj <0.05 were used to determine statistical significance.

Immune infiltration, copy number alteration and gene mutation analysis of SLC2A2 in GC. The infiltration of immune cells was analyzed using quantification of the tumor immune contexture from human RNA-seq data (QUANTISEQ from the 'Immunedeconv' R package; version 2.0.3, icbi.i-med.ac.at/software/quantiseq/doc/). The Pearson correlation coefficient was calculated to explore the correlation between immune cell infiltration and *SLC2A2* expression (13). To explore the correlation between the expression levels of *SLC2A2* and different immune infiltrating cells in GC, the Tumor Immune Estimation Resource 2.0 database (http://timer.cistrome.org/) was used to analyze the association between *SLC2A2* and immune infiltration levels, and a Cox proportional hazard

model was constructed. The copy number alterations of *SLC2A2* in GC and the gene mutation status of SLC2A2 in GC were investigated using cBioPortal (version 5.4.7; https://www.cbioportal.org/).

Immune checkpoint, MYC targets, TMB, MSI and chemotherapeutic response analysis of SLC2A2 in GC. Further analysis was conducted to assess the association between *SLC2A2* expression and six major immune checkpoints, namely glucocorticoid-induced tumor necrosis factor-related [GITR; TNFR superfamily 18 (TNFRSF18)] protein, programmed cell death ligand 1 (PD-L1; CD274), programmed cell death 1 (PDCD1), cytotoxic T-lymphocyte associated protein 4 (CTLA4), sialic acid binding Ig-like lectin 15 (SIGLEC15) and signal regulatory protein α (SIRPα). MYC targets, TMB and MSI were examined to assess the effectiveness of immunotherapy using 'ggstatsplot' (version 4.0.2; https://github.com/IndrajeetPatil/ggstatsplot) and 'GSVA' (version 1.34.0; https://www.bioconductor.org/packages/release/bioc/vignettes/GSVA/inst/doc/GSVA.html). The Spearman's correlation coefficient was calculated to explore the correlation between MYC targets/TMB/MSI score and *SLC2A2* expression. To predict the chemotherapeutic response associated with *SLC2A2* expression, the IC_{50} score was analyzed based on Genomics of Drug Sensitivity in Cancer (release-8.2; https://www.cancerrxgene.org/) (14). The 'pRRophetic' package (version 0.5; https://github.com/paulgeeleher/pRRophetic) was used for prediction and the IC_{50} score was calculated using ridge regression.

Survival prognosis analysis of SLC2A2. Based on the clinical data from TCGA (https://tcga-data.nci.nih.gov/tcga/), Kaplan-Meier curves were used to investigate the association between survival prognosis and *SLC2A2* expression in GC using the 'survival' package (version 3.2-10; https://cran.r-project.org/package=survival). OS, disease-specific survival (DSS) and progression-free interval (PFI) of the patients divided into low and high *SLC2A2* expression groups based on the median of *SLC2A2* expression as the cutoff were compared. *SLC2A2* expression and corresponding clinical variables were evaluated using univariate and multivariate Cox regression analysis to determine independent prognostic factors for survival. Clinical information such as age, sex, TNM stage and the R0 grade for complete resection of residual tumor was incorporated. To elucidate the prognostic effect of *SLC2A2* in GC, subgroup analysis was conducted. The Sankey diagram, prognostic nomogram and corresponding calibration plots were generated using 'survival' (version 3.2-10; https://cran.r-project.org/package=survival) and 'RMS' (version 6.2-0; https://cran.r-project.org/web/packages/rms/index.html) packages to predict the OS at 1, 4 and 6 years. Discrimination was quantified using the concordance index and the accuracy of the nomogram was evaluated by comparing observed rates and nomogram-predicted probabilities.

Validation of differential SLC2A2 expression and predictive values. To validate *SLC2A2* expression and its predictive value, *SLC2A2* expression in normal gastric tissue from healthy individuals and GC tissues was compared using the Human Protein Atlas (HPA) database (proteinatlas.org/). A total of two microarray datasets, GSE38749 and GSE84437, were downloaded from the Gene Expression Omnibus (GEO) database (ncbi.nlm.nih.gov/geo/) to analyze the association between expression levels of *SLC2A2* and clinical characteristics in GC, including survival status, age, T stage and N stage (15,16). Kaplan-Meier plotter (2022 version; kmplot.com/analysis/) was then used to verify whether *SLC2A2* affects GC prognosis. The log-rank P-value and hazard ratio (HR) with 95% confidence intervals were calculated. An automatic cut-off value for high or low *SLC2A2* expression was determined by the Kaplan-Meier plotter, and the GC mRNA dataset and corresponding clinical information analyzed by Kaplan-Meier plotter came from three databases, including TCGA, GEO and European Genome-phenome Archive.

Immunohistochemistry (IHC). A GC tissue microarray (TMA; cat. no. D046St01) was purchased from Xi'an Bioaitech Co., Ltd. The GC tissues were fixed in 4% paraformaldehyde (room temperature; <24 h), immobilized in paraffin and sectioned at 4 μm. The TMA contained 46 samples, including 40 samples of GC and 6 mild gastritis samples from gastric mucosa adjacent to cancer. IHC of the TMA was carried out according to standard procedures (17). Briefly, the IHC application solution kit (cat. no. 13079S; Cell Signaling Technology, Inc.) was used for staining. After being heated to 60°C for 1 h, the TMA was deparaffinized in turpentine oil type biological tablet transparent agent three times for 10 min each, then dipped in 99.5% anhydrous ethanol (C2H60; cat. no. C15188908; Macklin Inc.) and 95% ethanol (C2H60; cat. no. C13799050; Macklin, Inc.) twice for 10 min each. The TMA was transferred to EDTA buffer (pH 6.0) by microwave heating for antigen retrieval. Microwave heating was performed at medium-high for 4 min, high for 5 min and then another 10 min at medium-high, then washed with distilled water (dH_2O) after cooling. The TMA was washed with dH_2O three times for 5 min each, immersed in 3% hydrogen peroxide for 20 min, then washed with dH_2O, Tris-Buffered Saline and 0.1% Tween-20 (TBST). The slide was blocked with 20% (1X) animal-free blocking solution (cat. no. 15019S; Cell Signaling Technology, Inc.) at room temperature for 2 h and incubated with primary antibody (anti-SLC2A2; 1:500; cat. no. 66889-1-Ig; Proteintech Group, Inc.) overnight at 4°C, followed by a 30-min incubation with 2 drops (100 μl) secondary antibody (SignalStain® Boost IHC Detection Reagent; HRP; mouse; cat. no. 8125S; Cell Signaling Technology, Inc.) at room temperature. A three-step washing procedure with TBST was followed by SignalStain® 3,3'-diaminobenzidine staining (cat. no. 8059S; Cell Signaling Technology, Inc.). The TMA was mounted and observed in three randomly selected fields of view (light microscope; magnification, x400; Pannoramic MIDI; 3DHISTECH, Ltd.) to calculate the average optical density. IHC intensity was quantified using Fiji ImageJ (version 2.0.0; National Institutes of Health) by calculating the integrated and mean integrated optical density (IOD) (IOD/area).

Cell lines. The GES-1 normal gastric mucosal epithelial cell line and three types of GC cell lines (AGS, HGC-27 and NCI-N87) were obtained from BeNa Culture Collection; Beijing Beina Chunglian Institute of Biotechnology. GES-1 cells were maintained in DMEM (Wuhan Servicebio

Technology Co., Ltd.) containing 10% FBS (Gibco; Thermo Fisher Scientific, Inc.). AGS and NCI-N-87 cells were cultured in RPMI-1640 medium (Gibco; Thermo Fisher Scientific, Inc.) containing 10% FBS, while HGC-27 cells were maintained in RPMI-1640 medium (Gibco; Thermo Fisher Scientific, Inc.) containing 20% FBS. All cells were cultured at 37˚C in a humidified atmosphere containing 5% CO_2.

Reverse transcription-quantitative PCR (RT-qPCR). Total cellular RNA was isolated from GES-1, AGS, HGC-27 and NCI-N87 cells using the RNApure Tissue & Cell kit (cat. no. CW0560S; CoWin Biosciences), and cDNA was synthesized using a UnionScript First-strand cDNA Synthesis Mix for qPCR (cat. no. SR511; Beijing Genesand Biotech Co., Ltd.). The reverse transcription conditions were 37˚C for 2 min, 55˚C for 15 min and 85˚C for 5 min using the T100 Thermo Cycler (Bio-Rad Laboratories, Inc.). RT-qPCR was performed using a QuanStudioTM 5 Real-Time PCR instrument (Thermo Fisher Scientific, Inc.) using GS AntiQ qPCR SYBR Green Fast Mix (cat. no. SQ410; Beijing Genesand Biotech Co., Ltd.). GAPDH (forward primer, 5'-GAAGGTGAAGGTCGGAGTC-3' and reverse primer, 5'-GAAGATGGTGATGGGATTTC-3') was used as the internal control. The human SLC2A2 qPCR primers were: Forward, 5'-ATTGCTCCAACCGCTCTCA-3' and reverse, 5'-ATGGCTCGCACACCAGAC-3'. The thermocycling conditions were as follows: Initial denaturation at 95˚C for 3 min, followed by 40 cycles of 95˚C for 5 sec and 60˚C for 15 sec, and melting curve at 95˚C for 15 sec, 60˚C for 1 min and 95˚C for 15 sec. The relative gene expression of *SLC2A2* was calculated as the FC using the $2^{-\Delta\Delta Cq}$ method (18) and GraphPad Prism (version 8.0; Dotmatics).

Statistical analysis. Log_2 transformation was used to normalize gene expression data. For analysis of *SLC2A2* expression, the Wilcoxon rank-sum test was used. Using univariate and multivariate Cox regression models, the HR and 95% CI of various clinical features were determined. Pearson and Spearman's coefficients were calculated to explore the correlation between immune cell infiltration, immune checkpoints and MYC/TMB/MSI score and *SLC2A2* expression. The statistical difference of QUANTISEQ Scores was tested using the Kruskal-Wallis test. Bonferroni post hoc tests were used for post hoc comparisons. The potential relationship between *SLC2A2*, prognosis and immunotherapy efficacy of GC related to copy number variation and gene mutation was analyzed using cBioPortal (version 5.4.7; https://www.cbioportal.org/) to perform a comprehensive analysis of *SLC2A2* alterations in GC. The time-dependent receiver operating characteristic (ROC) curve was used to verify the sensitivity and specificity of *SLC2A2* in the diagnosis of GC. Kaplan-Meier curves, Kruskal-Wallis test with Dunn's post hoc test and the log-rank test were used to analyze survival differences. According to different clinical parameters, the high and low *SLC2A2* expression groups determined by median were compared with the Kruskal-Wallis test to validate *SLC2A2* expression and its predictive value for the survival function. Data analysis was conducted using R software (version 3.6.3; https://www.r-project.org/about.html). The IOD was calculated using Fiji ImageJ (version 2.0.0; National Institutes of Health) and data were analyzed using one-way ANOVA with Tukey's post hoc test. Data are presented as the mean ± SD. qPCR was performed three times independently. A two-sided P<0.05 was considered to indicate a statistically significant difference.

Results

Differential SLC2A2 expression in GC and other types of cancer. The sequencing data of a total of 210 normal samples and 414 GC samples were extracted from GTEx and TCGA databases. Among them, the normal samples included 174 samples from healthy individuals and 36 samples from normal gastric mucosal tissue adjacent to cancer. *SLC2A2* expression was downregulated in most types of tumor, such as breast invasive carcinoma (P<0.001), cholangiocarcinoma (P<0.001), lymphoid neoplasm diffuse large B-cell lymphoma (P<0.05), kidney chromophobe (P<0.001), acute myeloid leukemia (P<0.001), lung squamous cell carcinoma (P<0.05), ovarian serous cystadenocarcinoma (P<0.001), prostate adenocarcinoma (P<0.001), skin cutaneous melanoma (P<0.001), thyroid carcinoma (P<0.001), thymoma (P<0.001), uterine corpus endometrial carcinoma (P<0.01) and testicular germ cell tumors (P<0.001; Fig. 1A), but upregulated in six tumor types compared with the normal tissues, including stomach adenocarcinoma/GC (P<0.001), colon adenocarcinoma (P<0.001), esophageal carcinoma (P<0.001), glioblastoma multiforme (P<0.001), kidney renal clear cell carcinoma (P<0.001) and pancreatic adenocarcinoma (P<0.05; Fig. 1A). *SLC2A2* expression was unchanged in several tumors, including adrenocortical carcinoma, bladder urothelial carcinoma, and cervical squamous cell carcinoma and endocervical adenocarcinoma (Fig. 1A). Based on |logFC|>2 and P.adj<0.05 thresholds, 1,471 DEGs, including of 1,465 significantly upregulated and six significantly downregulated genes, were identified (Fig. 1B). In addition, according to the |logFC| value, six significantly DEGs were selected from each of the upregulated (APOA4, AFP, APOA1, APOA2, VCX2 and AC115619.1) and downregulated genes (BOK-AS1, AC105460.1, CALB1, CLCA4, TMPRSS11B and CALCA) in descending order. A correlation heat map was constructed to display the association between *SLC2A2* and the top 12 significantly upregulated and downregulated DEGs (Fig. 1C).

Functional enrichment analysis of SLC2A2 in GC. DEG-associated functional enrichment analysis was conducted. According to KEGG pathway and GO term functional enrichment analysis (Fig. 2A and B), for BPs, *SLC2A2*-related DEGs were enriched predominantly in 'sensory perception of smell', 'chylomicron assembly', 'detection of chemical stimulus involved in sensory perception', 'plasma lipoprotein particle assembly' and 'detection of chemical stimulus involved in sensory perception of smell'. For CCs, DEGs were primarily related to 'high-density lipoprotein particle', 'chylomicron', 'triglyceride-rich plasma lipoprotein particle', 'blood microparticle' and 'very-low-density lipoprotein particle'. For the MFs, DEGs were mostly involved in 'olfactory receptor activity', 'intermembrane lipid transfer activity', 'lipoprotein particle receptor binding', 'cholesterol transporter activity' and 'intermembrane cholesterol transfer activity' (Fig. 2C). In addition, 'olfactory transduction', 'cholesterol metabolism',

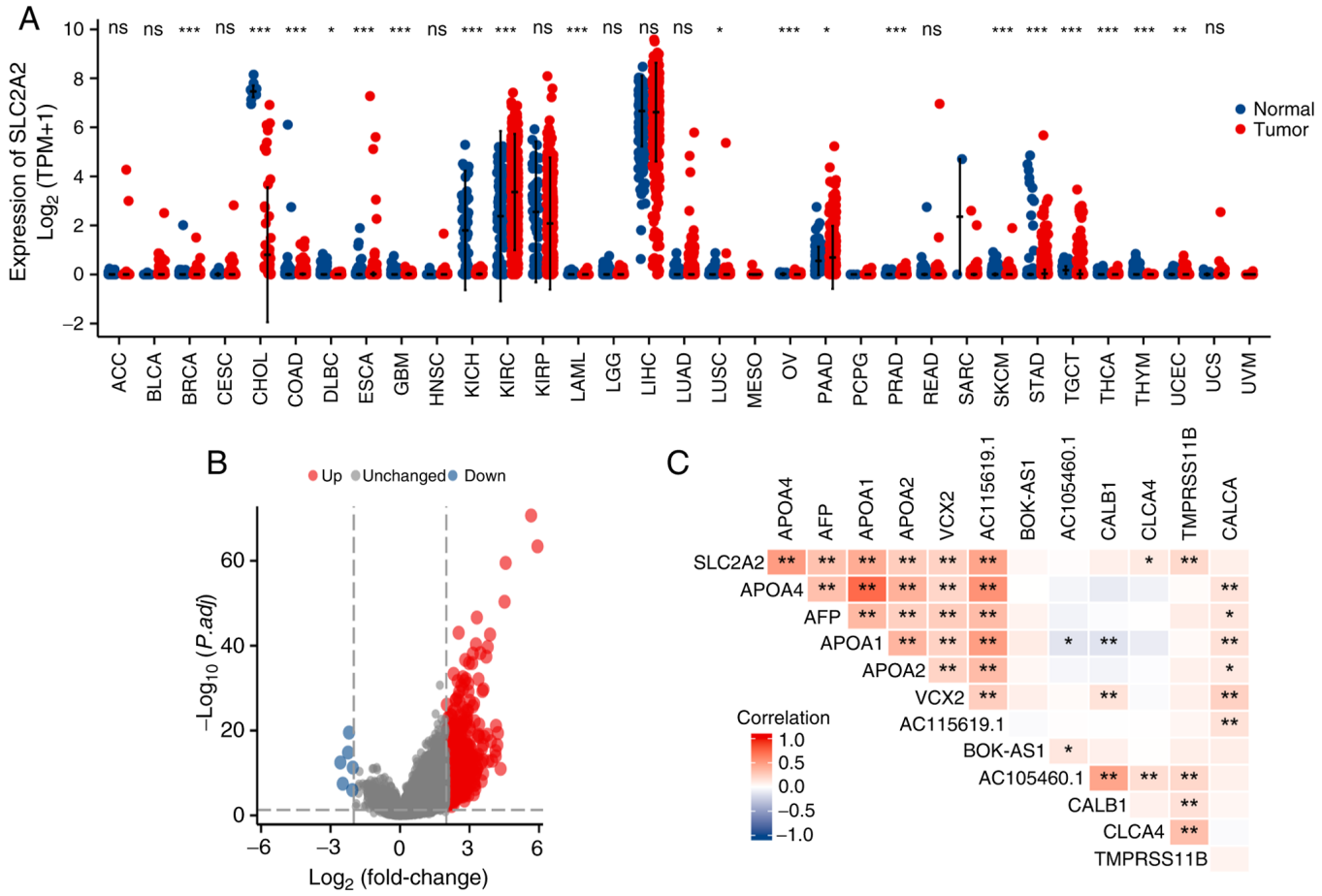

Figure 1. Differential expression of *SLC2A2* in cancer types and GC. (A) *SLC2A2* expression in pan-cancers and normal tissues. (B) Differentially expressed analysis between the high and low *SLC2A2* expression groups of GC determined by median expression levels of *SLC2A2*. (C) Correlation between *SLC2A2* and the top 12 significantly upregulated and downregulated genes. *P<0.05, **P<0.01, ***P<0.001, tumor vs. normal, and for the correlation between two genes. GC, gastric cancer; ns, not significant; P.adj, adjusted P-value; SLC2A2, solute carrier family 2 member 2; TPM, transcripts per million.

'fat digestion and absorption', 'complement and coagulation cascades' and 'vitamin digestion and absorption' were significantly enriched in the KEGG pathway analysis (Fig. 2D).

GSEA of GO enrichment analysis, Reactome pathway analysis and Wiki pathways analysis between SLC2A2 high expression and low expression levels for latent biological functions. To determine the latent functions of *SLC2A2* in patients with GC, GSEA was conducted based on false discovery rate q-values <0.25 and P.adj<0.05. According to GO enrichment analysis, 'sterol transfer activity', 'sterol transporter activity', 'lipoprotein particle receptor binding', 'lipid transfer activity' and 'cholesterol binding' were significantly enriched in association with high *SLC2A2* expression (Fig. 3A). However, 'DNA N glycosylase activity', 'prenyltransferase activity', 'MHC class I protein binding', 'superoxide generating NADPH oxidase activator activity' and 'CXCR chemokine receptor binding' were significantly enriched in association with low *SLC2A2* expression (Fig. 3B). According to the Reactome pathway analysis, 'chylomicron assembly', 'plasma lipoprotein assembly', 'GRB2 SOS provides linkage to MAPK signaling for integrins', 'P130CAS linkage to MAPK signaling for integrins' and 'metabolism of fat soluble vitamins' were significantly enriched in association with increased *SLC2A2* expression (Fig. 3C), and 'regulation of NFκB signaling', 'signaling by NOTCH1 HD domain mutants in cancer', 'SUMOylation of immune response proteins', 'repression of Wnt target genes' and 'mitochondrial iron sulfur cluster biogenesis' were significantly enriched in association with decreased *SLC2A2* expression (Fig. 3D). Furthermore, the association between Wiki pathways and *SLC2A2* expression was investigated based on the C2 collection from the Molecular Signatures Database. 'Lipid particles composition', 'metabolic pathway of LDL HDL and TG including diseases', 'statin inhibition of cholesterol production', 'PPARα pathway' and 'folate metabolism' were significantly enriched in association with high *SLC2A2* expression (Fig. 3E), and 'amplification and expansion of oncogenic pathways as metastatic traits', 'apoptosis modulation by HSP70', 'cancer immunotherapy by CTLA4 blockade', 'development of pulmonary dendritic cells and macrophage subsets' and 'aerobic glycolysis' were significantly enriched in association with low *SLC2A2* expression (Fig. 3F). These results indicated that *SLC2A2* expression was associated with dynamic alteration of inflammatory chemokines, oxidative stress, lipid metabolism, inflammatory reaction, immune regulation and the tumor immune microenvironment.

Association between SLC2A2 and immune infiltration and mutation types of SLC2A2 by mutation count and alteration frequency. *SLC2A2* expression and immune cell infiltration

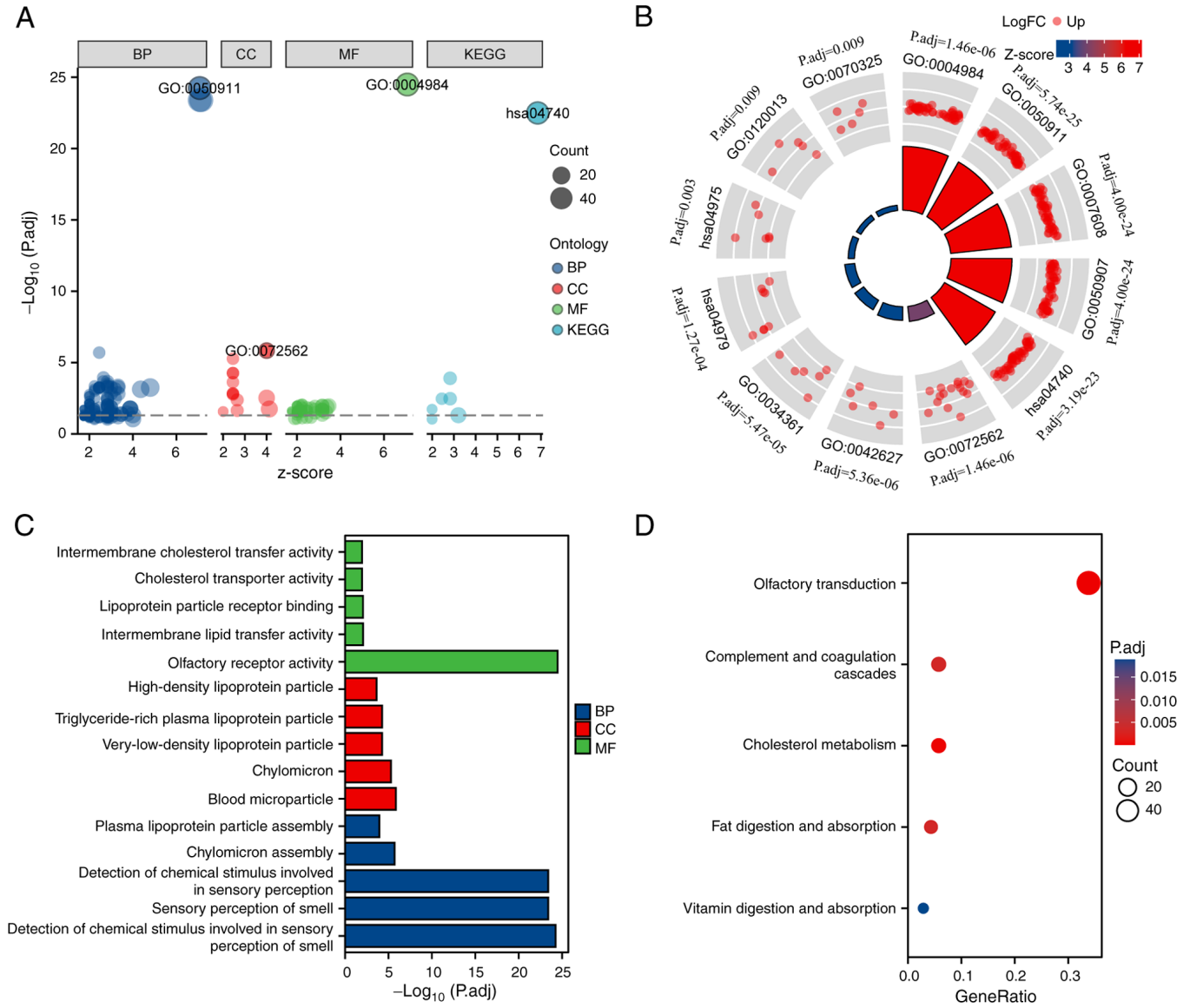

Figure 2. Functional enrichment analysis of *SLC2A2* in gastric cancer. (A) KEGG pathway and GO term functional enrichment analysis of *SLC2A2*. (B) Circleplot of functional enrichment analysis of *SLC2A2*. (C) GO term enrichment analysis. (D) KEGG pathway enrichment analysis of *SLC2A2*. BP, biological process; CC, cellular component; FC, fold-change; GO, Gene Ontology; KEGG, Kyoto Encyclopedia of Genes and Genomes; MF, molecular function; P.adj, adjusted P-value; SLC2A2, solute carrier family 2 member 2; P.adj, adjusted P-value.

levels in GC were analyzed. QUANTISEQ revealed that neutrophils (P=0.003) and M2 macrophages (P=0.045) were significantly increased in patients with high *SLC2A2* expression, whereas M1 macrophages (P=0.037) were significantly decreased (Fig. 4A-C), although the correlations were weak. The distribution of QUANTISEQ immune score in GC tissue was divided into high expression group and low expression group according to the median expression value of *SLC2A2*, and data for 32 normal samples of gastric mucosa adjacent to cancer from the same patients were extracted from TCGA as the normal group for this immune score. GC and normal tissues exhibited significant differences in M1 macrophages (P<0.001), monocytes (P<0.001), neutrophils (P<0.05) and $CD4^+$ T cells (P<0.05), while M2 macrophages were markedly different (0.05≤P<0.1; Fig. 4D). The analysis of putative copy number alterations showed that the expression of *SLC2A2* was related to missense point mutations, with the highest mutation count found in the diploid, indicating the gene mutations of *SLC2A2* in GC may contribute to poor prognosis and immunotherapy might be effective for this patients with high expression level of *SLC2A2* (Fig. 4E). Mutation analysis showed that SLC2A2 was highly amplified in GC, and the highest amplification rate of 6.28% was found in TCGA Firehose Legacy cohort (Fig. 4F). The multivariate Cox proportional hazard model of immune subsets of GC revealed that *SLC2A2* primarily affected the prognosis of patients by affecting the infiltration of macrophages and B cells in the immune microenvironment of GC (Table I).

Correlation between immune checkpoints, MYC, TMB, MSI and IC_{50} and SLC2A2 expression. Further analyses were conducted to investigate the relationship between *SLC2A2* expression and the immune checkpoints of GC, namely GITR (TNFRSF18), PD-L1 (CD274), PDCD1, CTLA4, SIGLEC15

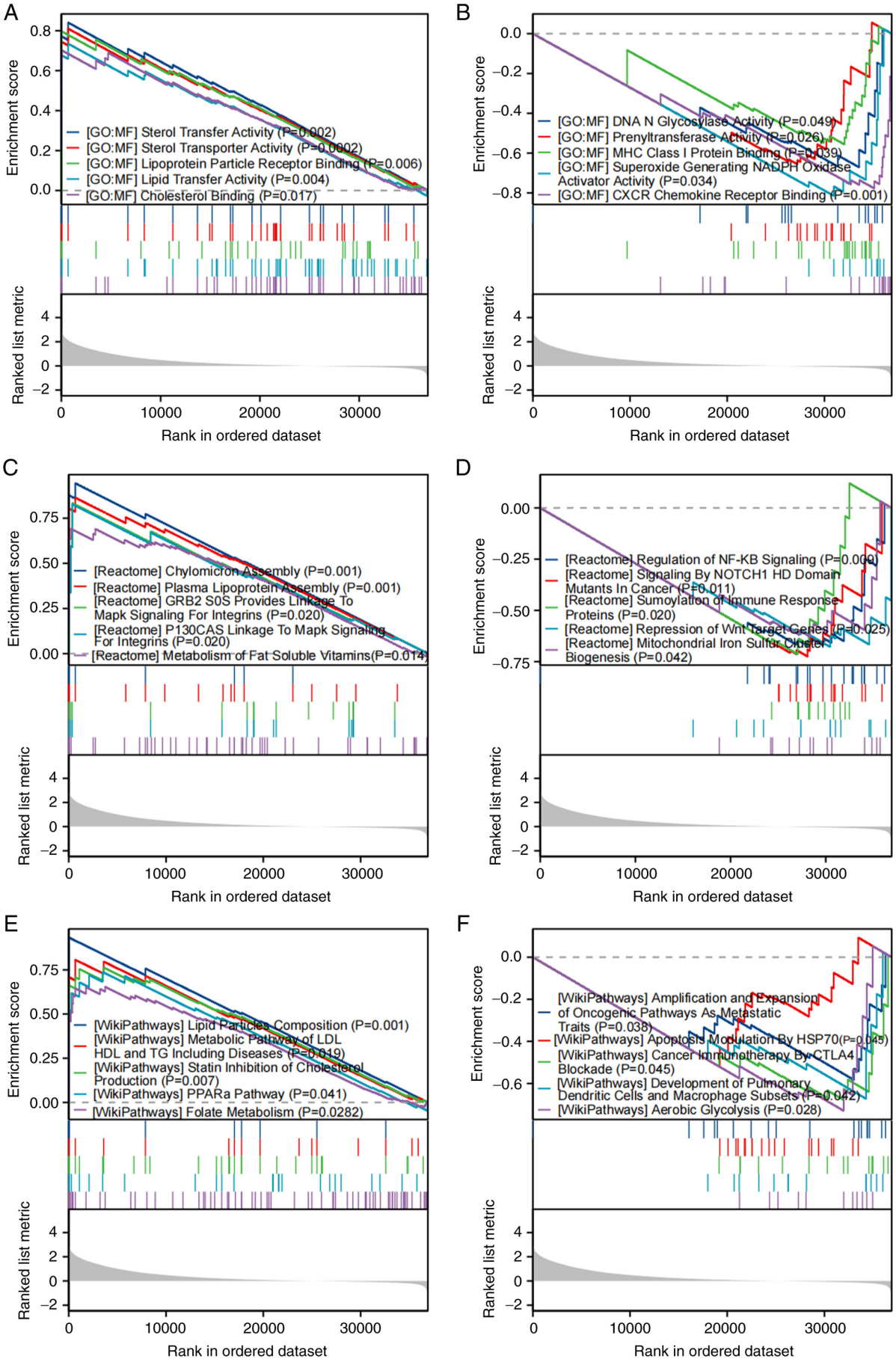

Figure 3. Gene set enrichment analysis of solute carrier family 2 member 2. (A) GO term analysis for high *SLC2A2* expression. (B) GO term analysis for low *SLC2A2* expression. (C) Reactome analysis for high *SLC2A2* expression. (D) Reactome analysis for low *SLC2A2* expression. (E) Wiki pathway analysis for high *SLC2A2* expression. (F) Wiki pathway analysis for low *SLC2A2* expression. GO, Gene Ontology; MF, molecular function.

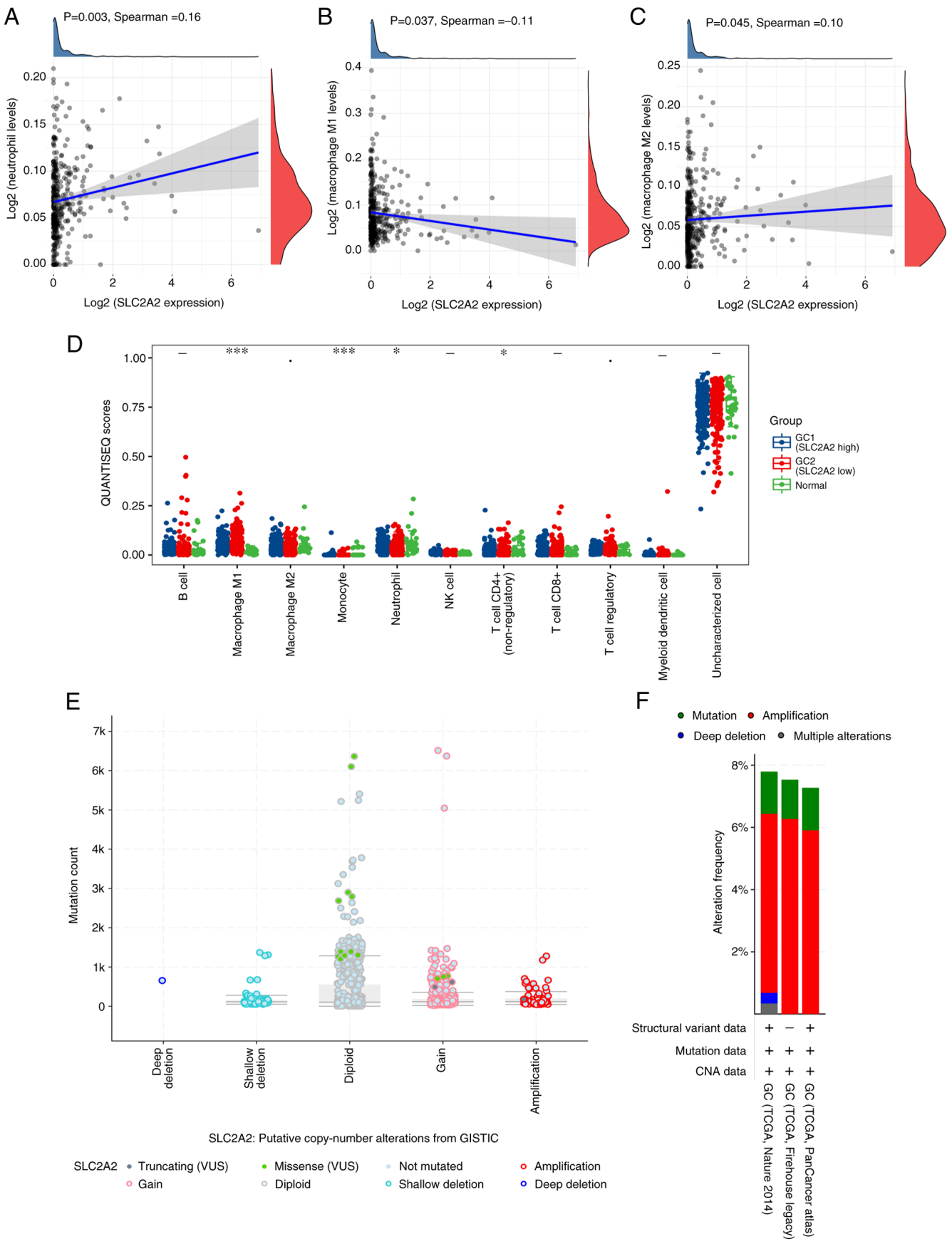

Figure 4. Association between *SLC2A2* expression and immune infiltration. Relationships between *SLC2A2* expression and (A) neutrophils, (B) M1 macrophages, (C) M2 macrophages and (D) QUANTISEQ immune scores. (E) Association between copy number alterations, mutation types and mutation count of *SLC2A2* in GC. (F) Analysis of the gene mutations of *SLC2A2* in GC. *P<0.05, ***P<0.001, Ÿ0.05≤P<0.1, high expression of *SLC2A2* vs. low expression of *SLC2A2 vs*. normal groups in GC. GC, gastric cancer; NK, natural killer; QUANTISEQ, quantification of the tumor immune contexture from human RNA-seq data; SLC2A2, solute carrier family 2 member 2; STAD, stomach adenocarcinoma; TCGA, The Cancer Genome Atlas; GISTIC, Genomic Identification of Significant Targets in Cancer; VUS, variants of uncertain significance; CNA, copy number alteration.

Table I. Cox proportional hazard model of gastric cancer immune subsets.

Characteristic	Regression coefficient	95% CI	Hazard ratio	P-value
SLC2A2 expression	0.283	1.004-1.753	1.327	0.047[a]
Age	0.037	1.017-1.059	1.038	<0.001[b]
Male sex	0.172	0.788-1.791	1.188	0.411
Ethnicity (black)	0.288	0.542-3.278	1.333	0.531
Ethnicity (white)	0.169	0.722-1.944	1.185	0.502
Stage 2	0.783	0.970-4.937	2.189	0.059
Stage 3	1.167	1.504-6.859	3.212	0.003[c]
Stage 4	1.725	2.071-15.225	5.615	0.001[c]
B cell	3.078	1.097-10,548.852	107.592	0.046[a]
$CD8^+$ T cell	-0.986	0.018-7.598	0.373	0.521
$CD4^+$ T cell	-5.023	0.000-1.586	0.007	0.073
Macrophage	7.317	45.703-49,588.633	1,505.436	<0.001[b]
Neutrophil	-5.242	0.000-2.818	0.005	0.102
Dendritic cell	1.960	0.486-103.643	7.099	0.152

[a]P<0.05, [b]P<0.001 and [c]P<0.01. SLC2A2, solute carrier family 2 member 2.

and SIRPα. *SLC2A2* expression was positively correlated with SIGLEC15 (r=0.151; P=0.003) and SIRPα (r=0.116; P=0.025) and inversely correlated with GITR (r=-0.115; P=0.025) and PD-L1 (r=-0.105, P=0.042) expression (Fig. 5A and B), although the correlations were weak. However, lower MYC targets (r=-0.13; P=0.010), TMB (r=-0.14; P=0.012) and MSI score (r=-0.21; P=0.000195) were associated with increased *SLC2A2* expression, although the correlations were weak (Fig. 5C-E). The aforementioned data showed that with the increase of *SLC2A2* expression level, the expression of immune checkpoint SIGLEC15 and SIRPa increased, indicating that GC was more likely to exhibit immune escape, and thus, further spread and metastasize, while the levels of MYC targets, TMB score and MSI score decreased with the high expression of *SLC2A2,* resulting in a worse immunotherapy effect in GC (19,20). The results indicated that high expression of *SLC2A2* may lead to poor immunotherapy efficacy in GC.

To evaluate the association between drug sensitivity and *SLC2A2* expression, the IC_{50} score was determined based on Genomics of Drug Sensitivity in Cancer (12). IC_{50} scores of the most common chemotherapy drugs for GC were significantly increased in the high *SLC2A2* expression group as follows: 5-Fluorouracil (P=0.0097), doxorubicin (P=0.00047), A-770041 (P=0.01), etoposide (P=0.0098), mitomycin C (P=0.0028), parthenolide (P=0.012), saracatinib (P=0.01), imatinib (P=0.015) and salubrinal (P=0.021) (Fig. 6).

Association between SLC2A2 and GC prognosis. The effect of *SLC2A2* on GC prognosis was assessed using Kaplan-Meier analysis. High *SLC2A2* expression was associated with worse prognosis in patients with GC with respect to OS (HR, 1.46; 95% CI, 1.05-2.03; P=0.024), DSS (HR, 1.59; 95% CI, 1.05-2.43; P=0.03) and PFI (HR, 1.46; 95% CI, 1.03-2.08; P=0.036) (Fig. 7A-C). According to univariate analysis, OS was significantly associated with high *SLC2A2* expression (P=0.024), age >65 years (P=0.005), T3 stage compared with T1&T2 stage (P=0.016), T4 stage compared with T1&T2 stage (P=0.028), M1 stage compared with M0 stage (P=0.004), R1&R2 residual tumor (P<0.001), N1 stage compared with N0 stage(P=0.049) and N3 stage compared with N0 stage (P<0.001; Fig. 7D). However, there was no significant relationship between OS and sex (0.188) or N2 stage compared with N0 stage (P=0.06) of GC (Fig. 7D). Multivariate regression analysis with the same variables demonstrated that GC could be independently prognosticated by *SLC2A2* (HR, 1.707; 95% CI, 1.155-2.521; P=0.007; Fig. 7E). The association between TNM stage and *SLC2A2* expression is shown in the Sankey diagram (Fig. 7F). Additionally, subgroup analyses were performed based on variables identified in the multivariate analysis. For OS rates, patients with GC with high *SLC2A2* expression had a significantly worse prognosis when analyzing subgroups of patients based on age >65 years (P=0.013), male sex (P=0.023), N0 stage (P=0.008), diffuse histological type (P=0.042), R0 residual tumor (P=0.015) and primary therapy outcome of complete response (P=0.039; Fig. 8A). For DSS rates, high *SLC2A2* expression was associated with a worse prognosis in the R0 residual tumor (P=0.013), age >65 years (P=0.029) and no reflux history (P=0.041) subgroups (Fig. 8B). T4 stage (P=0.027), R0 residual tumor (P=0.028) and no reflux history (P=0.04) subgroups of patients exhibited significant differences in PFI rates between the high and low *SLC2A2* expression groups (Fig. 8C).

The association among *SLC2A2* expression, survival time and risk scores was calculated to determine the predictive value, and the results showed that with the increasing expression level of *SLC2A2*, the risk score of patients was higher based on the heat map, scatter plot and risk curve (Fig. 9A). The ROC curve was used to verify the sensitivity and specificity of *SLC2A2* in the diagnosis of GC. The ROC curve had an area under the curve (AUC) of 0.692 based

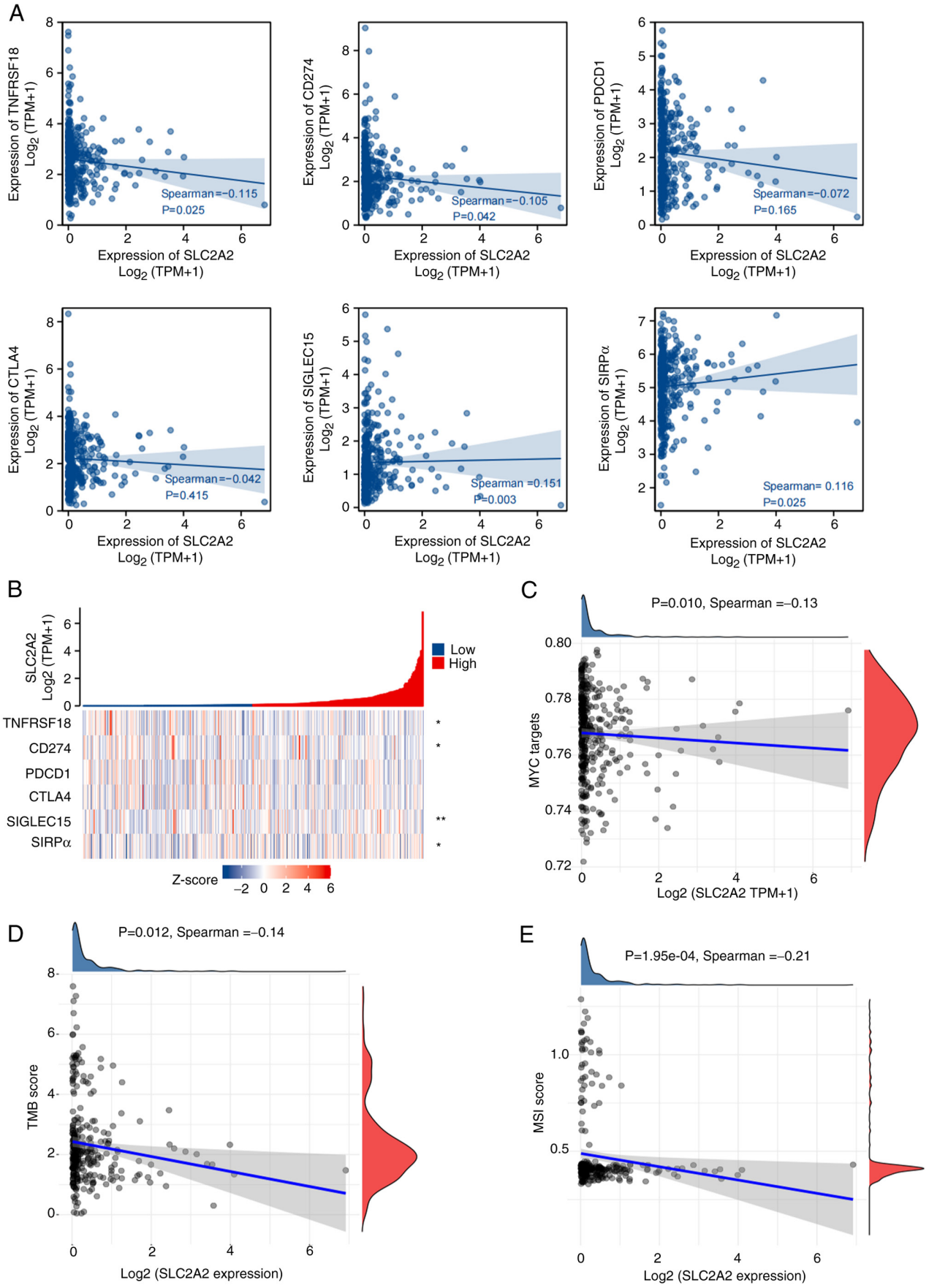

Figure 5. Spearman's correlation between immune checkpoints, MYC, TMB and MSI and *SLC2A2* expression. (A) Correlation between *SLC2A2* and immune checkpoints. (B) Heatmap of *SLC2A2* co-expression with immune checkpoints. (C) Association between *SLC2A2* and MYC targets. (D) Association between *SLC2A2* and TMB score. (E) Association between *SLC2A2* and MSI score. CTLA4, cytotoxic T-lymphocyte associated protein 4; MSI, microsatellite instability; PDCD1, programmed cell death 1; SIGLEC15, sialic acid binding Ig-like lectin 15; SIRPα, signal regulatory protein α; SLC2A2, solute carrier family 2 member 2; TMB, tumor mutation burden; TNFRSF18, TNFR superfamily 18; TPM, transcripts per million.

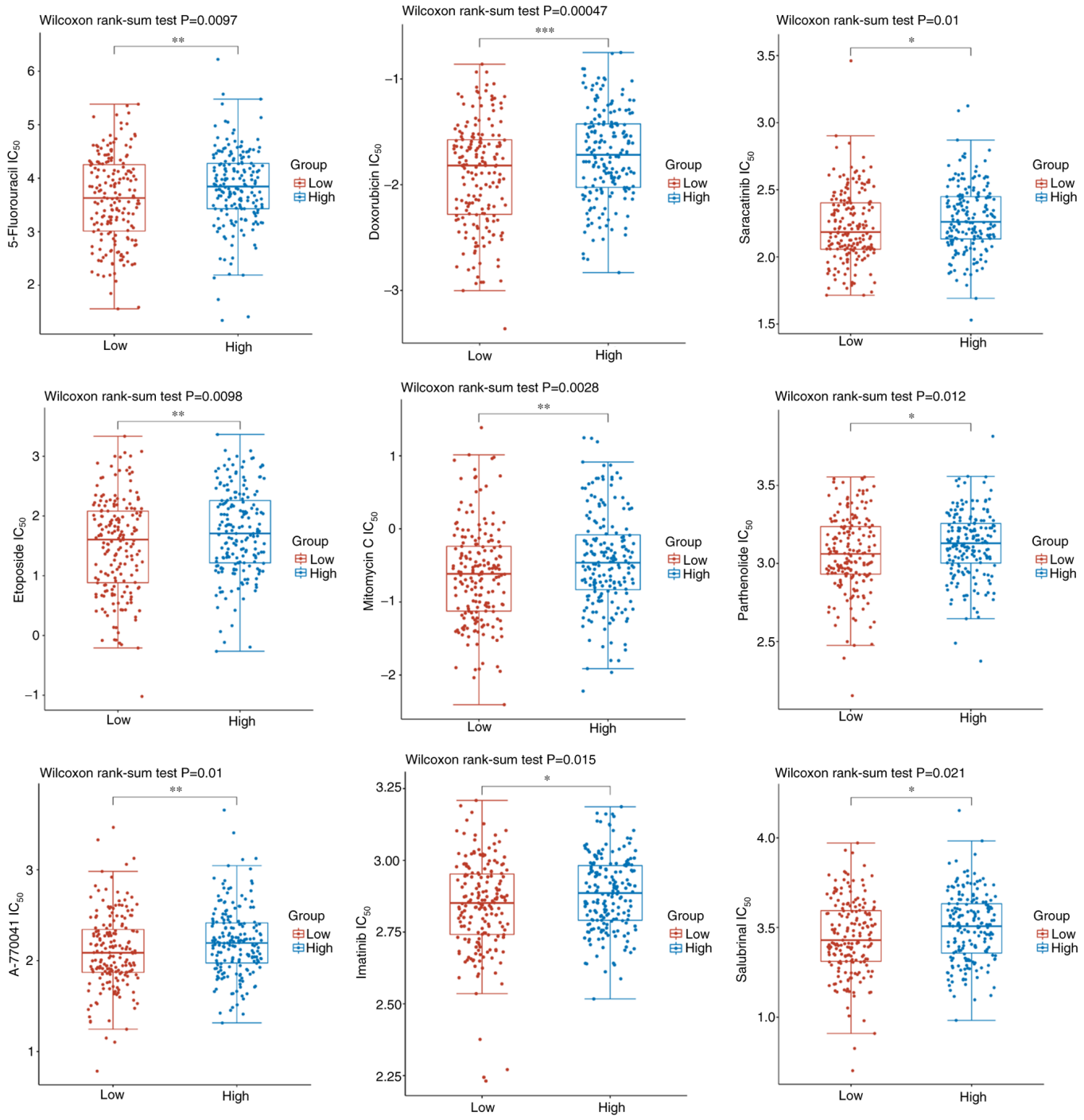

Figure 6. Analysis of IC_{50} and *SLC2A2* expression. SLC2A2, solute carrier family 2 member 2. *P<0.05, **P<0.01, ***P<0.001, high expression of *SLC2A2* vs. low expression of *SLC2A2* in GC.

on the clinical data of 624 patients with GC obtained from GTEx and TCGA (Fig. 9B) and the AUC for OS rates was 0.548, 0.612 and 0.786 at 1, 4 and 6 years, respectively (Fig. 9C).

Finally, a nomogram model was constructed, its predictive power was confirmed and its accuracy quantified. The concordance index for the nomogram based on the clinical variables, including *SLC2A2* expression, age, sex, T stage, N stage, M stage and the presence of residual tumor, was calculated as 0.707 (95% CI, 0.681-0.733; Fig. 10A). According to the calibration plots, the predicted probability was consistent with the observed outcome (Fig. 10B).

Validation of SLC2A2 expression and its predictive value. To validate the differential expression of *SLC2A2*, a comparison was made between healthy and GC tissues using the HPA database. GC tissues (medium staining, moderate intensity) exhibited higher levels of SLC2A2 protein than normal tissues (low staining, weak intensity; Fig. 11A). For further analyses, two microarray datasets, GSE38749 and GSE84437, and the corresponding clinical data of patients

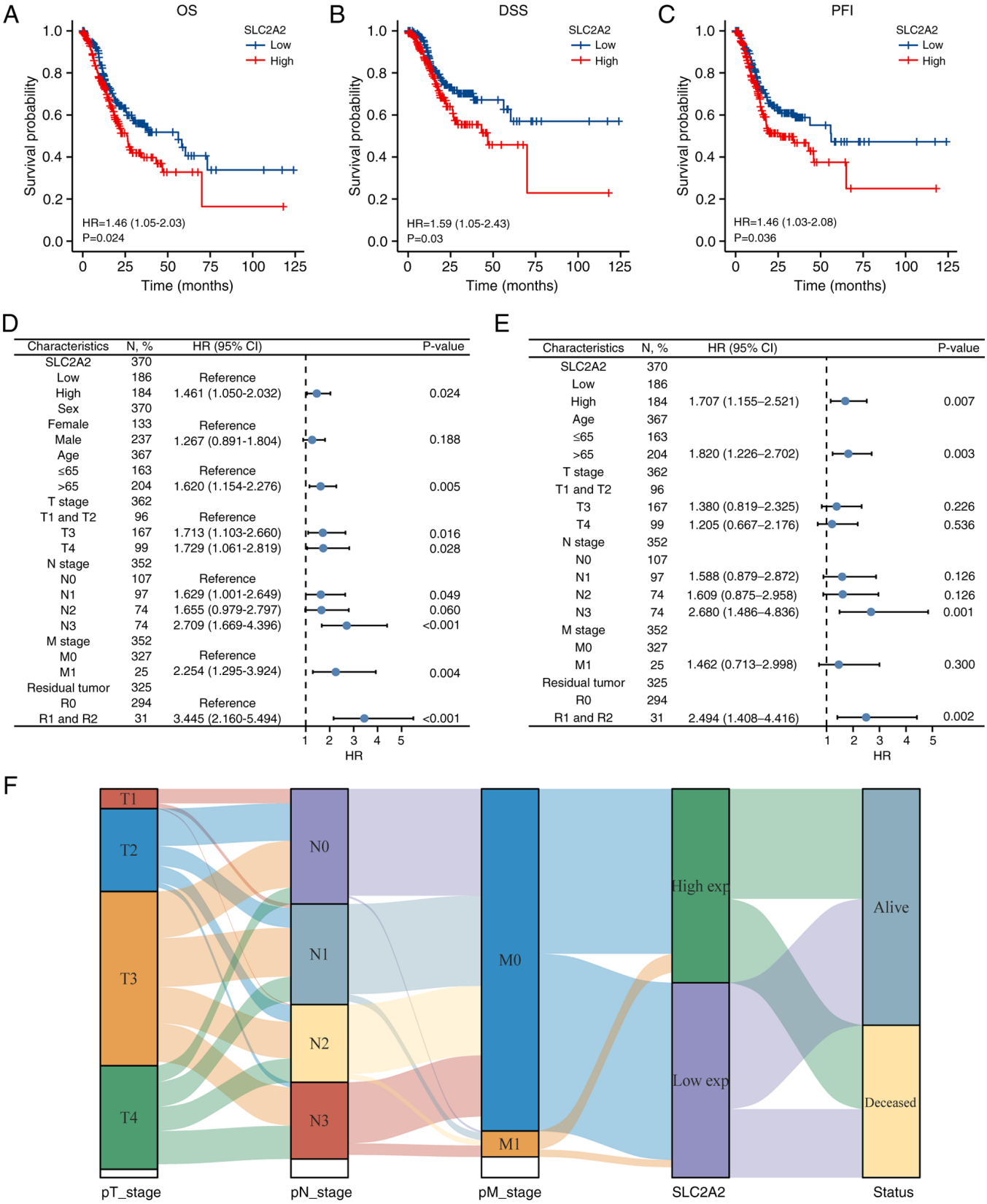

Figure 7. Association between *SLC2A2* and survival prognosis in gastric cancer. (A) OS. (B) DSS. (C) PFI. (D) Univariate and (E) multivariate Cox regression analysis of OS. (F) Sankey diagram of the association between TNM stage classification, high and low *SLC2A2* expression, and survival status. DSS, disease-specific survival; exp, expression HR, hazard ratio; OS, overall survival; PFI, progression-free interval; SLC2A2, solute carrier family 2 member 2.

with GC were obtained from the GEO database. Patients with GC were grouped according to survival status; the deceased group exhibited significantly higher levels of *SLC2A2* than the alive group (P=0.04), based on the GSE38749 dataset (Fig. 11B). Kaplan-Meier survival analysis revealed an association between high *SLC2A2* expression and poorer

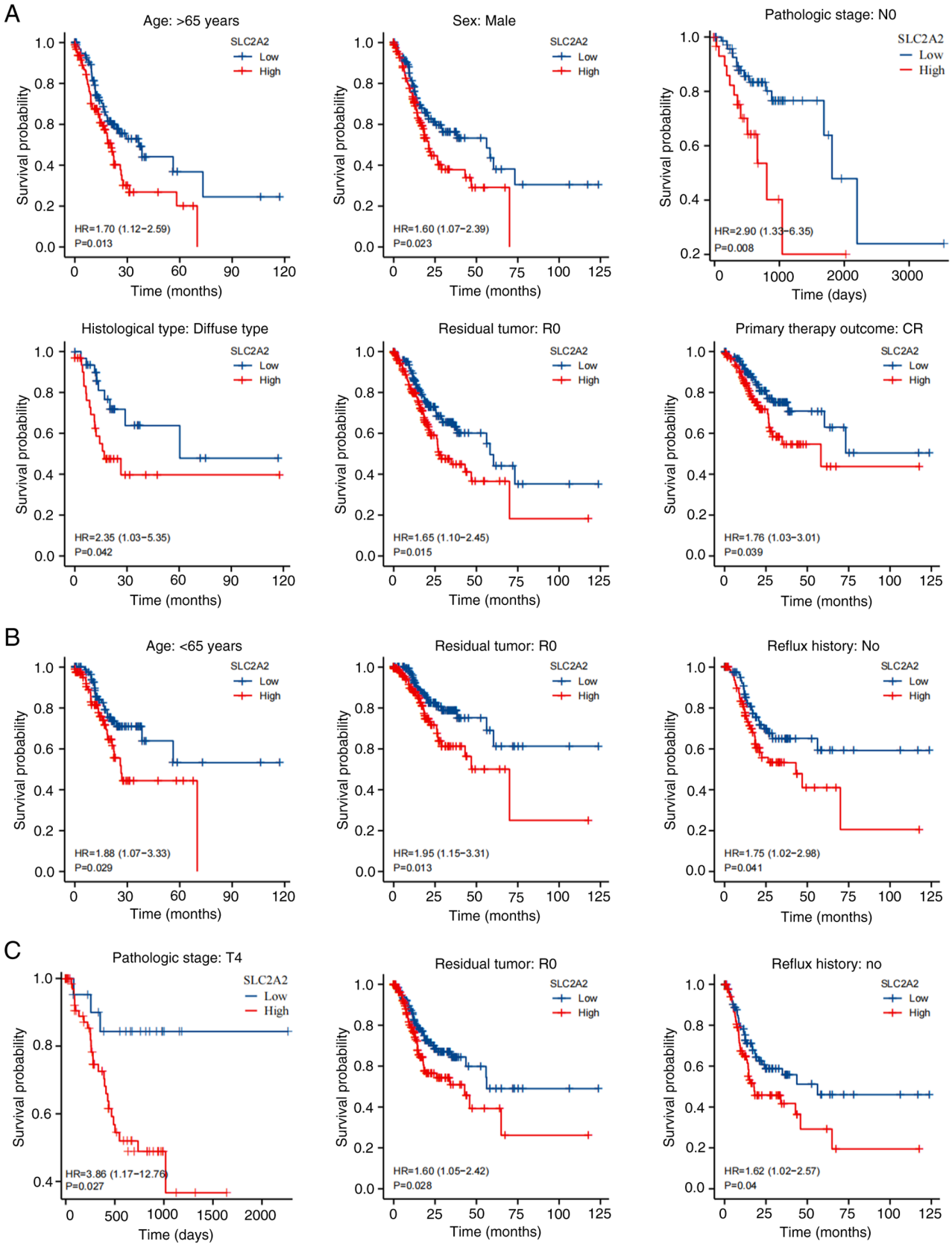

Figure 8. Subgroup analysis of *SLC2A* expression levels in gastric cancer based on clinical variables. Subgroup analysis of (A) overall survival, (B) disease-specific survival and (C) progression-free interval. SLC2A2, solute carrier family 2 member 2; HR, hazard ratio; CR, complete response.

prognosis in GC (HR, 5.35; 95% CI, 1.31-21.95; P=0.02; Fig. 11C). For the GSE84437 dataset, subgroup analysis was performed according to age, T stage and N stage. Wilcoxon and Kruskal-Wallis tests confirmed that *SLC2A2* expression varied significantly with age (>65 vs. ≤65 years; P=0.0094), T3 stage compared with T1&T2 stage (P=0.019), N1 stage

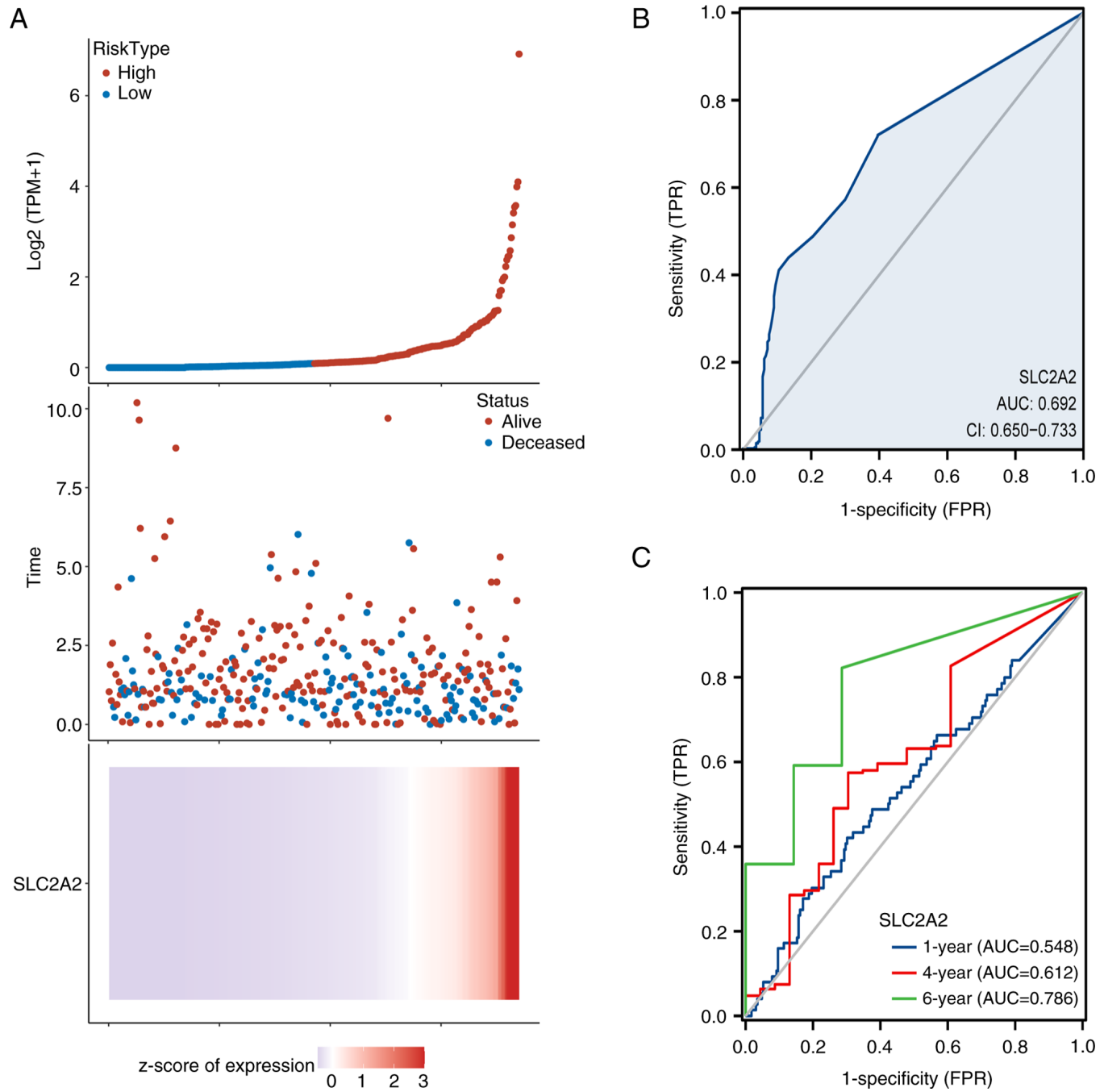

Figure 9. Analysis of the predictive value of *SLC2A2* expression in GC. (A) Association between *SLC2A2* expression, survival time, survival status and risk score in GC. (B) ROC curves of *SLC2A2* in the diagnosis of GC. (C) Time-dependent ROC curves for overall survival prediction. AUC, area under the curve; FPR, false positive rate; GC, gastric cancer; ROC, receiver operating characteristic; SLC2A2, solute carrier family 2 member 2; TPM, transcripts per million; TPR, true positive rate.

compared with N0 stage (P=0.011) and N2&N3 stage compared with N0 stage (P<0.01) (Fig. 11D-F). The effect of *SLC2A2* on GC prognosis was verified using Kaplan-Meier analysis. High *SLC2A2* expression was associated with a worse prognosis in patients with GC with respect to OS (HR, 1.49; 95% CI, 1.22-1.83; P=0001), progression-free survival (HR, 1.45; 95% CI, 1.15-1.82; P=0.0014) and post-progression survival (HR, 1.47; 95% CI, 1.15-1.88; P=0.0017; Fig. 11G-I). In terms of OS rates, patients with GC with high *SLC2A2* expression had a significantly worse prognosis in the analysis of N3 stage (HR, 1.81; P=0.04), male (HR, 1.49; P=0.0022) and female (HR, 1.54; P=0.015) subgroups of patients (Fig. 11J-L).

Immunohistochemical analysis of SLC2A2. The TMA contained 46 samples, including 40 samples of GC and 6 samples of adjacent gastric tissues (Table II). The GC samples comprised two T2, 19 T3 and 19 T4 stage samples and seven N0, five N1, eight N2 and 20 N3 samples (Table II). IHC staining showed that SLC2A2 was primarily expressed in the cytoplasm and membrane of normal human gastric mucosal epithelial and GC cells (Fig. 12A and D).

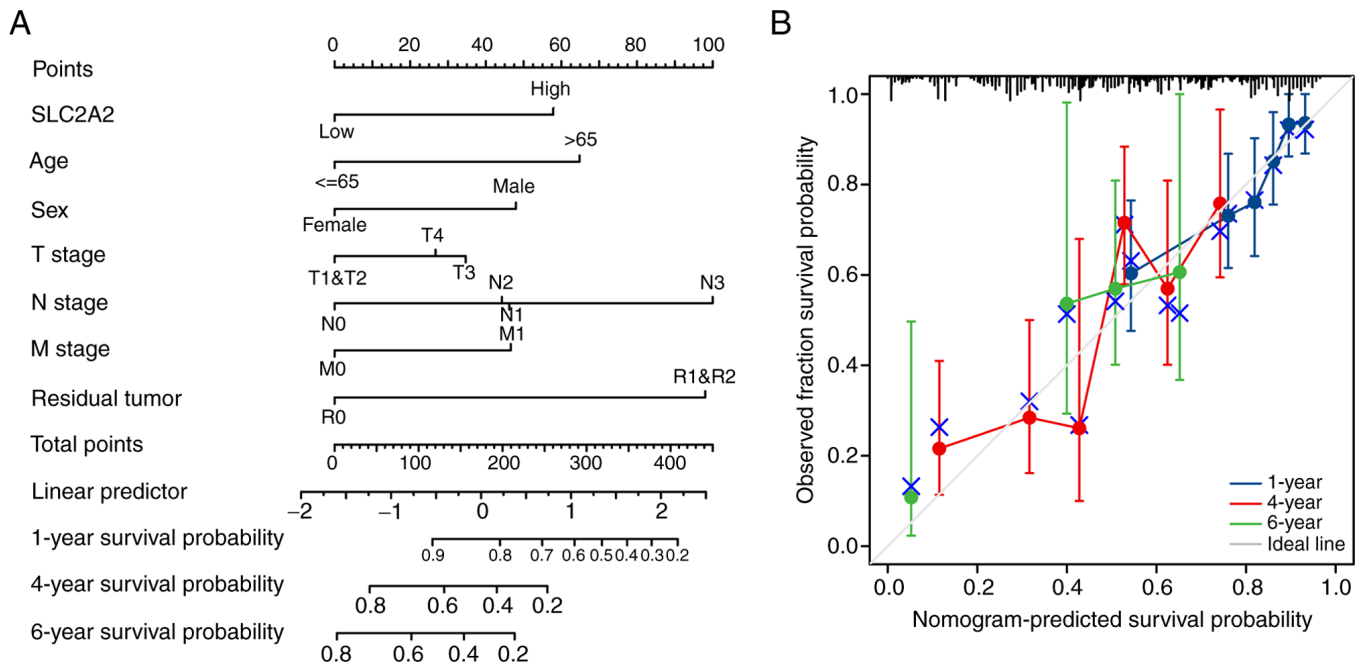

Figure 10. Construction of *SLC2A2*-associated prognosis model. (A) OS of gastric cancer predicted by nomogram. (B) Calibration plots for OS prediction. OS, overall survival; SLC2A2, solute carrier family 2 member 2.

IHC staining showed that there were significant differences in SLC2A2 expression among different T and N stages of GC (Fig. 12A-J). SLC2A2 expression in T4 GC was significantly higher than that in T3 (P=0.027) and T2 (P=0.0485) GC (Fig. 12E), and SLC2A2 expression in N3 GC was significantly higher than that in N2 GC (P=0.0264; Fig. 12J). IHC demonstrated that SLC2A2 expression in mild gastritis tissues was significantly higher than that in GC tissues of different stages, including N and T stages (P<0.0001).

RT-qPCR analysis of SLC2A2. To verify the differential expression of *SLC2A2* in normal gastric mucosal epithelial cells and GC cell lines, RT-qPCR was performed. *SLC2A2* expression in GC cells with different degrees of differentiation was significantly different (Fig. 12K). Among them, HGC-27 cells were derived from relatively differentiated GC tissues, NCI-N87 cells were isolated from male patients with GC complicated with liver metastasis and AGS cells were derived from an untreated primary GC excision fragment. All three types of GC cells had different degrees of malignant transformation potential (21-23). *SLC2A2* expression was the highest in NCI-N87 cells and significantly differed from that in GES-1 (P=0.0174), AGS (P=0.026) and HGC-27 cells (P=0.0009), indicating that the expression of *SLC2A2* was related to the degree of malignancy.

Discussion

Despite improvements in clinical diagnosis and surgical techniques, chemotherapy resistance and metastasis are major challenges in improving the prognosis of malignant GC (24). Therefore, identifying effective prognostic biomarkers and targets associated with immunological interventions is a GC research hotspot (8,25). Under hypoxic conditions, tumor cells require large amounts of metabolites and nutrients to meet their high metabolic energy demand (26). *SLC2A2*, an important member of the SLC2A family, is mainly responsible for transferring glucose into cells and may be involved in tumor development and invasion (10). In the present study, *SLC2A2* was evaluated as a prospective prognostic marker and chemotherapeutic target for GC.

In pan-cancer differential *SLC2A2* expression analysis, *SLC2A2* expression was considerably downregulated in most types of tumor but upregulated in GC, suggesting that *SLC2A2* may serve a different role in the occurrence and development of GC compared with other types of tumor. It was hypothesized that this was due to the continuous production of gastric acid and accumulation of lactic acid, which results in a lower pH and enhanced glycolytic metabolic activity in the GC microenvironment compared with other malignant tumors (27,28). GLUT, a promoter of the glycolytic pathway, is associated with the upregulation of glucose metabolism in cancer cells (29). Therefore, the expression of glucose transporters (GLUT1-3) in GC is higher than that in normal gastric mucosa (30). The functional enrichment analysis indicated that *SLC2A2* expression was associated with lipid metabolism. As part of tumor metabolic reprogramming, abnormal tumor lipid and glucose metabolism serve an important role in tumorigenesis, metastasis and prognosis (31-33). Numerous studies have demonstrated that tumor cells are characterized by deregulation of lipid metabolism, which has a regulatory effect on the tumor immune microenvironment (34-36).

Immune infiltration levels were examined in high and low *SLC2A2* expression GC cases using QUANTISEQ based on 10 immune cell subtypes and an uncharacterized cell. In the immunological correlation analysis between *SLC2A2* and 10 different immune cells, high immune infiltration of M2 macrophages and low immune infiltration of M1 macrophages

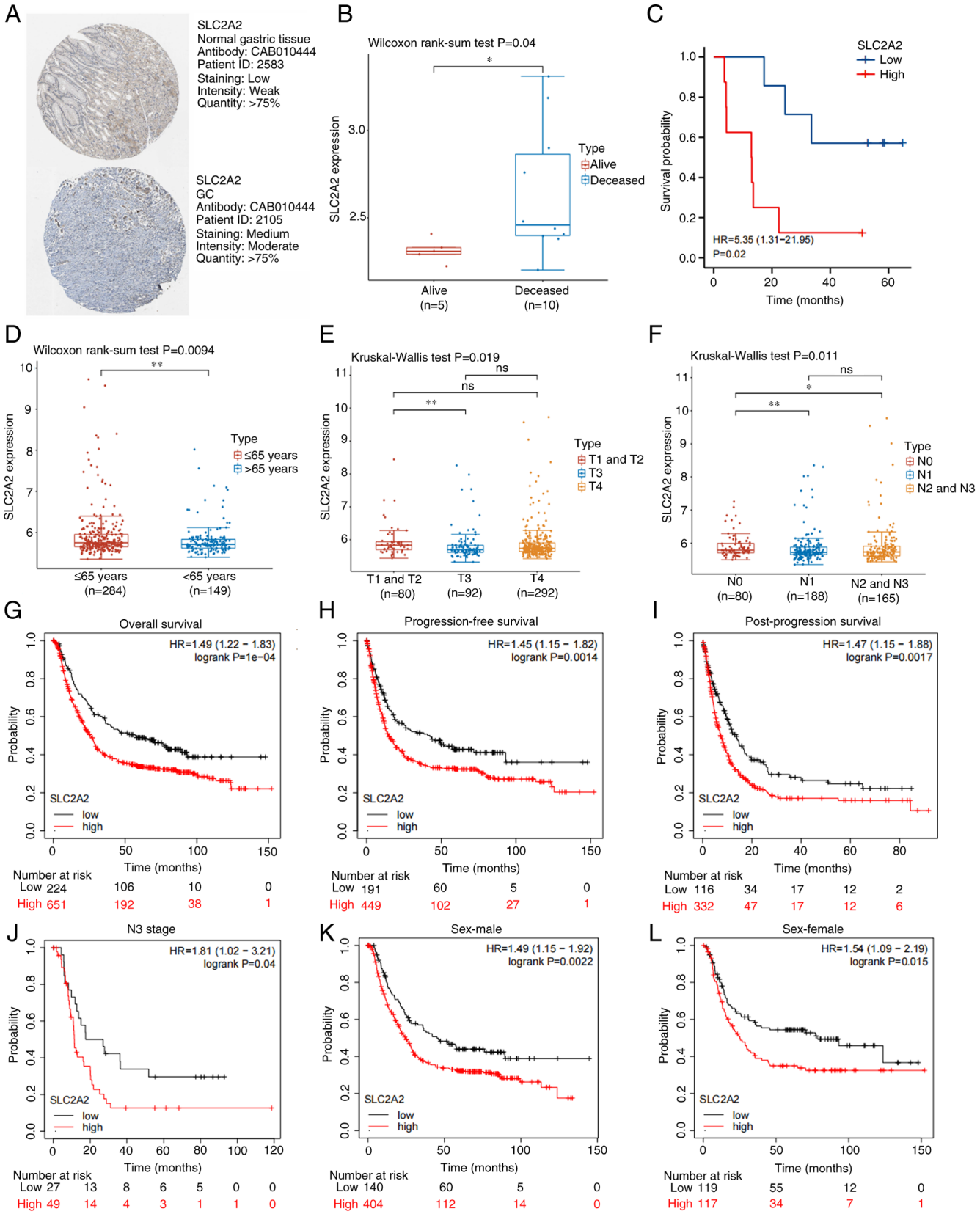

Figure 11. Validation of *SLC2A2* expression and its predictive value. (A) *SLC2A2* expression in normal and GC tissues derived from Human Protein Atlas database. (B) Association between *SLC2A2* expression and survival status based on GSE38749. (C) Association between *SLC2A2* expression and survival time based on GSE38749. (D) Association between *SLC2A2* expression and age based on GSE84437. (E) Association between *SLC2A2* expression and T stage based on GSE84437. (F) Association between *SLC2A2* expression and N stage based on GSE84437. (G) Association between *SLC2A2* expression and overall survival based on Kaplan-Meier plotter. (H) Association between *SLC2A2* expression and progression-free interval based on Kaplan-Meier plotter. (I) Association between *SLC2A2* expression and post-progression survival based on Kaplan-Meier plotter. (J) Association between *SLC2A2* expression and N3 stage based on Kaplan-Meier plotter. (K) Association between *SLC2A2* expression and sex-male based on Kaplan-Meier plotter. (L) Association between *SLC2A2* expression and sex-female based on Kaplan-Meier plotter. *P<0.05, **P<0.01, deceased vs. alive, >65 years vs. ≤65 years, T3 vs. T1 and T2, N1 vs. N0, and N2 and N3 vs. N0. GC, gastric cancer; HR, hazard ratio; SLC2A2, solute carrier family 2 member 2.

Table II. Baseline characteristics of 46 samples in the tissue microarray.

Characteristic	Number of samples	
	Gastric cancer	Adjacent gastric tissue
Pathology		
Mild gastritis	0	6
Gastric adenocarcinoma	40	0
Age, years		
≤65	26	4
>65	14	2
Sex		
Female	13	2
Male	27	4
T stage		
1	0	-
2	2	-
3	19	-
4	19	-
N stage		
0	7	-
1	5	-
2	8	-
3	20	-

-, not applicable.

were observed in patients with GC with high *SLC2A2* expression, although the correlations were weak. However, in the analysis of immune infiltration scores dividing GC into high expression and low expression groups based on the median expression of *SLC2A2*, only M1 macrophages showed significant differences, while M2 macrophages were markedly different between the high expression, low expression and normal groups of *SLC2A2*. We speculate that this is related to the small sample size of the normal group in this analysis of immune score and the weak correlation between *SLC2A2* and macrophages. As is well known, there is a dynamic balance of mutual inhibition between M1 polarization and M2 polarization of macrophages (37). Since the GC high expression group of *SLC2A2* has a lower level of M1 macrophage infiltration, we have reason to speculate that the infiltration level of M2 macrophages will also correspondingly increase, and increasing the sample size of the normal group for this immune score may enhance the significant relationship between *SLC2A2* and M2 macrophages. M2 macrophages are tumor-associated macrophages that promote the growth and metastasis of GC by secreting proteins or cytokines, such as chitinase 3 like 1 (37,38). Therefore, it was hypothesized that high *SLC2A2* expression mainly affects the prognosis of GC by increasing infiltration of M2 macrophages with tumor-promoting characteristics and reducing the infiltration of M1 macrophages with tumor-inhibiting characteristics. Furthermore, tumor-associated neutrophils induce the formation of neovessels via MMP-9, which influences tumor intravasation and angiogenesis (39-41). The high infiltration of M2 macrophages and neutrophils in tumors is associated with shorter OS, suggesting that high *SLC2A2* expression may contribute to immune suppression during cancer progression (42-44). A recent study also demonstrated that high solute carrier family 35 member A2 expression is associated with cell metabolism and macrophage polarization during progression of GC, indicating that the SLC family genes may promote cancer cell proliferation and angiogenesis by regulating the metabolic activity of immune and endothelial cells associated with GC cell metabolism in the tumor microenvironment (45).

A significant inverse correlation was observed between *SLC2A2* expression and immune checkpoints, including GITR and PD-L1. Immunotherapy has gained attention for its potential to improve the quality of life in patients with cancer, and TMB/MSI has been demonstrated as a key biomarker for immune checkpoint inhibitor response (46,47). The present study demonstrated that high *SLC2A2* expression was associated with decreased TMB and MSI scores in GC, which means that the immunotherapy effect will be worse. Therefore, the IC_{50} was used to evaluate the drug sensitivity associated with *SLC2A2* expression. The IC_{50} of the most commonly used chemotherapy drugs for GC, including 5-fluorouracil, doxorubicin and etoposide, was significantly increased the high *SLC2A2* expression group. Based on these findings, *SLC2A2* may be a useful target for personalized chemotherapy in GC.

Univariate and multivariate Cox regression analyses demonstrated that GC was independently prognosticated by *SLC2A2*. High *SLC2A2* expression is positively associated with higher OS for liver and breast cancer and other malignancies (10,11). However, the present study demonstrated that patients with GC with high *SLC2A2* levels had worse OS, DSS and PFI outcomes. It was hypothesized that this discrepancy may be attributed to *SLC2A2* serving a different role in the glucose and lipid metabolism of GC. GC cells have a different glucose metabolism compared with normal epithelial cells, and GLUT1 expression is associated with intestinal gastric carcinoma (48,49). In association with protein kinase B signaling, *SLC2A2* upregulation may enhance glucose transportation, leading to tumor growth and progression of GC (50,51). Apoptosis has been demonstrated to occur in cancer cells following glucose starvation in previous studies (52-54). Glucose is an important nutrient for tumor growth and low *SLC2A2* expression leads to GC cells receiving less nutrition and, consequently, entering the glucose starvation state, which induces cell apoptosis, and thus, serves an inhibitory role in GC (55,56).

IHC also demonstrated that SLC2A2 expression in mild gastritis tissues was significantly higher than that in GC tissues of different stages, including N and T stages. It was hypothesized that this may be due to abnormally enhanced metabolic reprogramming in GC, such as aerobic glycolysis and lipid metabolism, which may compensate for the promotion of glucose transport in normal gastric tissues adjacent to cancer tissues, thereby upregulating *SLC2A2* expression. Although normal mucosa samples derived from tissues adjacent to tumors in patients with GC were characterized, the specific regulatory mechanisms of high expression of *SLC2A2* in normal gastric

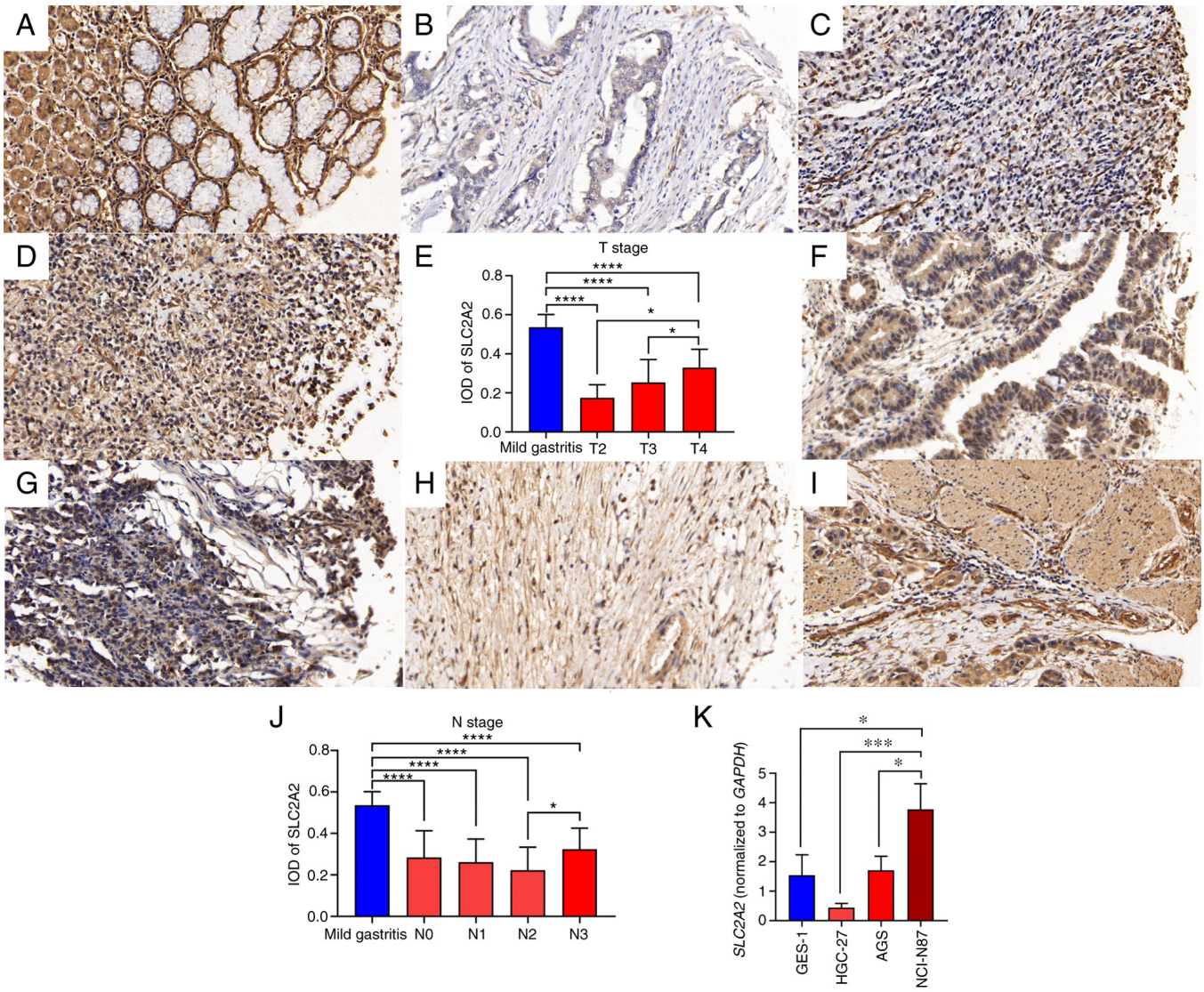

Figure 12. IHC staining and reverse transcription-quantitative PCR analysis of SLC2A2 in GC. (A) IHC staining of SLC2A2 in mild gastritis. (B) IHC staining of SLC2A2 in T2 stage of GC. (C) IHC staining of SLC2A2 in T3 stage of GC. (D) IHC staining of SLC2A2 in T4 stage of GC. (E) IOD analysis of SLC2A2 in different T stages. (F) IHC staining of SLC2A2 in the N0 stage of GC. (G) IHC staining of SLC2A2 in the N1 stage of GC. (H) IHC staining of SLC2A2 in the N2 stage of GC. (I) IHC staining of SLC2A2 in the N3 stage of GC. (J) IOD analysis of SLC2A2 in different N stages. (K) Quantification of SLC2A2 mRNA expression. Magnification, x400. *P<0.05, ***P<0.001, ****P<0.0001, T2 vs. mild gastritis, T3 vs. mild gastritis, T4 vs. mild gastritis, T4 vs. T2, T4 vs. T3, N0 vs. mild gastritis, N1 vs. mild gastritis, N2 vs. mild gastritis, N3 vs. mild gastritis, and N3 vs. N2. GC, gastric cancer; IHC, immunohistochemistry; IOD, integrated optical density; SLC2A2, solute carrier family 2 member 2.

mucosa and the formation and development of GC tissue require further study. Furthermore, a recent study found that under glucose starvation, cancer cells with high solute carrier family 7 member 11 expression underwent disulfidptosis due to excessive accumulation of disulfide, and treatment with GLUT inhibitor induced disulfidptosis of cancer cells and effectively inhibited tumor growth (57). As a key member of the GLUT family, *SLC2A2* may be an effective tool to improve the prognosis of GC by developing inhibitors of *SLC2A2* to induce disulfidptosis.

To conclude, *SLC2A2* may be a prospective prognostic marker and novel immunotherapy target for GC. The prediction model may improve the prognosis of patients with GC in clinical practice and *SLC2A2* may serve as a novel therapeutic target to provide novel immunotherapy plans for GC. However, the present study had limitations. The predictive efficacy of the model requires validation using GC samples from different stages and multicenter prospective studies. Furthermore, the potential molecular mechanism of action of *SLC2A2* in GC requires investigation.

Acknowledgements

Not applicable.

Funding

The present study was supported by Innovation Team and Talents Cultivation Program of National Administration of Traditional Chinese Medicine (grant no. ZYYCXTD-C-202208), Key-Area Research and Development Program of Guangdong Province-Modernization of Chinese Medicine in Lingnan (grant no. 2020B1111100011), Sanming Project of

Medicine in Shenzhen (grant no. SZZYSM202211002), and Guangdong Basic and Applied Basic Research Foundation (grant no. 2020A1515110947).

Availability of data and materials

The datasets used and/or analyzed during the current study are available from the corresponding author on reasonable request.

Authors' contributions

WZ, DZ and SS collected and analyzed data and prepared the figures. WZ, DZ, YW, SL and SZ carried out data collection and wrote the manuscript. XC, YH, YL, XH, YX and SG interpreted the data and revised the manuscript. HP and HL conceived and designed the study. HL and HP confirm the authenticity of all the raw data. All authors have read and approved the final manuscript.

Ethics approval and consent to participate

The present study was approved by the Medical Ethics Committee of Shenzhen Traditional Chinese Medicine Hospital (approval no. K2022-011-02; Shenzhen, China).

Patient consent for publication

Not applicable.

Competing interests

The authors declare that they have no competing interests.

References

1. Shi J, Fu H, Jia Z, He K, Fu L and Wang W: High expression of CPT1A predicts adverse outcomes: A potential therapeutic target for acute myeloid leukemia. EBiomedicine 14: 55-64, 2016.
2. Granito A, Marinelli S, Negrini G, Menetti S, Benevento F and Bolondi L: Prognostic significance of adverse events in patients with hepatocellular carcinoma treated with sorafenib. Ther Adv Gastroenterol 9: 240-249, 2016.
3. Xiaobin C, Zhaojun X, Tao L, Tianzeng D, Xuemei H, Fan Z, Chunyin H, Jianqiang H and Chen L: Analysis of related risk factors and prognostic factors of gastric cancer with bone metastasis: A SEER-based study. J Immunol Res 2022: 3251051, 2022.
4. Zhong Y, Kang W, Hu H, Li W, Zhang J and Tian Y: Lobaplatin-based prophylactic hyperthermic intraperitoneal chemotherapy for T4 gastric cancer patients: A retrospective clinical study. Front Oncol 13: 995618, 2023.
5. Yang J, Wei H, Liu M, Huang T, Fang X, Ren X, Huang T, Fang X, Ren X, Yuan H, *et al*: Prognostic biomarker HAMP and associates with immune infiltration in gastric cancer. Int Immunopharmacol 108: 108839, 2022.
6. Kim YH, Jeong DC, Pak K, Han ME, Kim JY, Liangwen L, Kim HJ, Kim TW, Kim TH, Hyun DW and Oh SO: SLC2A2 (GLUT2) as a novel prognostic factor for hepatocellular carcinoma. Oncotarget 8: 68381-68392, 2017.
7. Wei L, Sun J, Zhang N, Zheng Y, Wang X, Lv L, Liu J, Xu Y, Shen Y and Yang M: Noncoding RNAs in gastric cancer: Implications for drug resistance. Mol Cancer 19: 62, 2020.
8. Ding N, Zou Z, Sha H, Su S, Qian H, Meng F, Chen F, Du S, Zhou S, Chen H, *et al*: iRGD synergizes with PD-1 knockout immunotherapy by enhancing lymphocyte infiltration in gastric cancer. Nat Commun 10: 1336, 2019.
9. Shi H, Wang H, Pan J, Liu Z and Li Z: Comparing prognostic value of preoperative platelet indexes in patients with resectable gastric cancer. Sci Rep 12: 6480, 2022.
10. Mukhopadhyay P, Ye J, Anderson KM, Roychoudhury S, Rubin EH, Halabi S and Chappell RJ: Log-rank test vs MaxCombo and difference in restricted mean survival time tests for comparing survival under nonproportional hazards in immuno-oncology trials: A systematic review and meta-analysis. JAMA Oncol 8: 1294-1300, 2022.
11. Sperduto PW, Yang TJ, Beal K, Pan H, Brown PD, Bangdiwala A, Shanley R, Yeh N, Gaspar LE, Braunstein S, *et al*: Estimating survival in patients with lung cancer and brain metastases: An update of the graded prognostic assessment for lung cancer using molecular markers (lung-molGPA). JAMA Oncol 3: 827-831, 2017.
12. Abu N, Othman N, W Hon K, Nazarie WF and Jamal R: Integrative meta-analysis for the identification of hub genes in chemoresistant colorectal cancer. Biomark Med 14: 525-537, 2020.
13. Yoshikawa T, Inoue R, Matsumoto M, Yajima T, Ushida K and Iwanaga T: Comparative expression of hexose transporters (SGLT1, GLUT1, GLUT2 and GLUT5) throughout the mouse gastrointestinal tract. Histochem Cell Biol 135: 183-194, 2011.
14. Zhang Y, Liu Y, Huang J, Hu Z and Miao Y: Identification of new head and neck squamous cell carcinoma subtypes and development of a novel score system (PGSscore) based on variations in pathway activity between tumor and adjacent non-tumor samples. Comput Struct Biotechnol J 20: 4786-4805, 2022.
15. Pasini FS, Zilberstein B, Snitcovsky I, Roela RA, Mangone FR, Ribeiro UJ Jr, Nonogaki S, Brito GC, Callegari GD, Cecconello I, *et al*: A gene expression profile related to immune dampening in the tumor microenvironment is associated with poor prognosis in gastric adenocarcinoma. J Gastroenterol 49: 1453-1466, 2014.
16. Yoon SJ, Park J, Shin Y, Choi Y, Park SW, Kang SG, Son HY and Huh YM: Deconvolution of diffuse gastric cancer and the suppression of CD34 on the BALB/c nude mice model. BMC Cancer 20: 314, 2020.
17. Manning L, O'Rourke KI, Knowles DP, Marsh SA, Spencer YI, Moffat E, Wells GA and Czub S: A collaborative Canadian-United Kingdom evaluation of an immunohistochemistry protocol to diagnose bovine spongiform encephalopathy. J Vet Diagn Invest 20: 504-508, 2008.
18. Livak KJ and Schmittgen TD: Analysis of relative gene expression data using real-time quantitative PCR and the 2(-Delta Delta C(T)) method. Methods 25: 402-408, 2001.
19. Qin Y, Liu H, Huang X, Huang L, Liao L, Li J, Zhang L, Li W and Yang J: GIMAP7 as a potential predictive marker for pan-cancer prognosis and immunotherapy efficacy. J Inflamm Res 15: 1047-1061, 2022.
20. He J, Chen Z, Xue Q, Sun P, Wang Y, Zhu C and Shi W: Identification of molecular subtypes and a novel prognostic model of diffuse large B-cell lymphoma based on a metabolism-associated gene signature. J Transl Med 20: 186, 2022.
21. Li J, Xue H, Xiang Z, Song S, Yan R, Ji J, Zhu Z, Wei C and Yu Y: Genetic profiles affect the biological effects of serine on gastric cancer cells. Front Pharmacol 11: 1183, 2020.
22. Seeneevassen L, Giraud J, Molina-Castro S, Sifré E, Tiffon C, Beauvoit C, Staedel C, Mégraud F, Lehours P, Martin OCB, *et al*: Leukaemia inhibitory factor (LIF) inhibits cancer stem cells tumorigenic properties through hippo kinases activation in gastric cancer. Cancers (Basel) 12: 2011, 2020.
23. Ma J, Chen M, Wang J, Xia HH, Zhu S, Liang Y, Gu Q, Qiao L, Dai Y, Zou B, *et al*: Pancreatic duodenal homeobox-1 (PDX1) functions as a tumor suppressor in gastric cancer. Carcinogenesis 29: 1327-1333, 2008.
24. Wang Y, Fang Y, Zhao F, Gu J, Lv X, Xu R, Zhang B, Fang Z and Li Y: Identification of *GGT5* as a novel prognostic biomarker for gastric cancer and its correlation with immune cell infiltration. Front Genet 13: 810292, 2022.
25. Xu W, Sun T, Wang J, Li H, Chen B, Zhou Y, Wang T, Wang S, Liu J and Jiang H: LMO3 downregulation in PCa: A prospective biomarker associated with immune infiltration. Front Genet 13: 945151, 2022.
26. Zhao Y, Liu Y, Lin L, Huang Q, He W, Zhang S, Dong S, Wen Z, Rao J, Liao W and Shi M: The lncRNA MACC1-AS1 promotes gastric cancer cell metabolic plasticity via AMPK/Lin28 mediated mRNA stability of MACC1. Mol Cancer 17: 69, 2018.
27. Osumi H, Horiguchi H, Kadomatsu T, Tashiro K, Morinaga J, Takahashi T, Ikeda K, Ito T, Suzuki M, Endo M and Oike Y: Tumor cell-derived angiopoietin-like protein 2 establishes a preference for glycolytic metabolism in lung cancer cells. Cancer Sci 111: 1241-1253, 2020.

28. Luo F, Liu X, Yan N, Li S, Cao G, Cheng Q, Xia Q and Wang H: Hypoxia-inducible transcription factor-1alpha promotes hypoxia-induced A549 apoptosis via a mechanism that involves the glycolysis pathway. BMC Cancer 6: 26, 2006.
29. Kim SL, Lee ST, Min IS, Park YR, Lee JH, Kim DG and Kim SW: Lipocalin 2 negatively regulates cell proliferation and epithelial to mesenchymal transition through changing metabolic gene expression in colorectal cancer. Cancer Sci 108: 2176-2186, 2017.
30. Krawczyk M, Pastuch-Gawolek G, Pluta A, Erfurt K, Dominski A and Kurcok P: 8-hydroxyquinoline glycoconjugates: Modifications in the linker structure and their effect on the cytotoxicity of the obtained compounds. Molecules 24: 4181, 2019.
31. Wang N, Chen S, Zhang B, Li S, Jin F, Gao D, Liu H and Jiang Y: 8u, a pro-apoptosis/cell cycle arrest compound, suppresses invasion and metastasis through HSP90α downregulating and PI3K/Akt inactivation in hepatocellular carcinoma cells. Sci Rep 8: 309, 2018.
32. Zuo D, Li C, Liu T, Yue M, Zhang J and Ning G: Construction and validation of a metabolic risk model predicting prognosis of colon cancer. Sci Rep 11: 6837, 2021.
33. Cohnen J, Kornstädt L, Hahnefeld L, Ferreiros N, Pierre S, Koehl U, Deller T, Geisslinger G and Scholich K: Tumors provoke inflammation and perineural microlesions at adjacent peripheral nerves. Cells 9: 320, 2020.
34. Jiang N, Zhang Z, Chen X, Zhang G, Wang Y, Pan L, Yan C, Yang G, Zhao L, Han J and Xue T: Plasma lipidomics profiling reveals biomarkers for papillary thyroid cancer diagnosis. Front Cell Dev Biol 9: 682269, 2021.
35. Xu Y, Li H, Fan L, Chen Y, Li L, Zhou X, Li R, Cheng Y, Chen H and Yuan Z: Development of photosensitizer-loaded lipid droplets for photothermal therapy based on thiophene analogs. J Adv Res 28: 165-174, 2020.
36. Zheng M, Mullikin H, Hester A, Czogalla B, Heidegger H, Vilsmaier T, Vattai A, Chelariu-Raicu A, Jeschke U, Trillsch F, *et al*: Development and validation of a novel 11-gene prognostic model for serous ovarian carcinomas based on lipid metabolism expression profile. Int J Mol Sci 21: 9169, 2020.
37. Chen Y, Zhang S, Wang Q and Zhang X: Tumor-recruited M2 macrophages promote gastric and breast cancer metastasis via M2 macrophage-secreted CHI3L1 protein. J Hematol Oncol 10: 36, 2017.
38. Messex JK, Byrd CJ and Liou GY: Signaling of macrophages that contours the tumor microenvironment for promoting cancer development. Cells 9: 919, 2020.
39. Yuan J, Liang H, Li J, Li M, Tang B, Ma H, Xie X, Yin X, Zhang L and Ren Z: Peripheral blood neutrophil count as a prognostic factor for patients with hepatocellular carcinoma treated with sorafenib. Mol Clin Oncol 7: 837-842, 2017.
40. Li X, Li Y, Lu W, Chen M, Ye W and Zhang D: The tumor vessel targeting strategy: A double-edged sword in tumor metastasis. Cells 8: 1602, 2019.
41. Siracusano G, Tagliamonte M, Buonaguro L and Lopalco L: Cell surface proteins in hepatocellular carcinoma: From bench to bedside. Vaccines (Basel) 8: 41, 2020.
42. Brodsky AS, Khurana J, Guo KS, Wu EY, Yang D, Siddique AS, Wong IY, Gamsiz Uzun ED and Resnick MB: Somatic mutations in collagens are associated with a distinct tumor environment and overall survival in gastric cancer. BMC Cancer 22: 139, 2022.
43. Cao L, Che X, Qiu X, Li Z, Yang B, Wang S, Hou K, Fan Y, Qu X and Liu Y: M2 macrophage infiltration into tumor islets leads to poor prognosis in non-small-cell lung cancer. Cancer Manag Res 11: 6125-6138, 2019.
44. Meng J, Chen Y, Lu X, Ge Q, Yang F, Bai S, Liang C and Du J: Macrophages and monocytes mediated activation of oxidative phosphorylation implicated the prognosis and clinical therapeutic strategy of wilms tumour. Comput Struct Biotechnol J 20: 3399-3408, 2022
45. Huang Z, Yang H, Lao J and Deng W: Solute carrier family 35 member A2 (SLC35A2) is a prognostic biomarker and correlated with immune infiltration in stomach adenocarcinoma. PLoS One 18: e287303, 2023.
46. Chen L, Diao L, Yang Y, Yi X, Rodriguez BL, Li Y, Villalobos PA, Cascone T, Liu X, Tan L, *et al*: CD38-mediated immunosuppression as a mechanism of tumor cell escape from PD-1/PD-L1 blockade. Cancer Discov 8: 1156-1175, 2018.
47. Kim Y, Song S, Lee M, Swatloski T, Kang JH, Ko YH, Park WY, Jeong HS and Park K: Integrative genomic analysis of salivary duct carcinoma. Sci Rep 10: 14995, 2020.
48. Liu W, Yang LJ, Liu YL, Yuan DS, Zhao ZM, Wang Q, Yan Y and Pan HF: Dynamic characterization of intestinal metaplasia in the gastric corpus mucosa of Atp4a-deficient mice. Biosci Rep 40: BSR20181881, 2020.
49. Yuan LW, Yamashita H and Seto Y: Glucose metabolism in gastric cancer: The cutting-edge. World J Gastroenterol 22: 2046-2059, 2016.
50. Wang J, Fang Y and Liu T: TRIM32 promotes the growth of gastric cancer cells through enhancing AKT activity and glucose transportation. Biomed Res Int 2020: 4027627, 2020.
51. Kim WS, Kim YY, Jang SJ, Kimm K and Jung MH: Glucose transporter 1 (GLUT1) expression is associated with intestinal type of gastric carcinoma. J Korean Med Sci 15: 420-424, 2000.
52. Berthe A, Flament S, Grandemange S, Zaffino M, Boisbrun M and Mazerbourg S: Δ2-Troglitazone promotes cytostatic rather than pro-apoptotic effects in breast cancer cells cultured in high serum conditions. Cell Cycle 15: 3402-3412, 2016.
53. Go S, Kramer TT, Verhoeven AJ, Oude ER and Chang JC: The extracellular lactate-to-pyruvate ratio modulates the sensitivity to oxidative stress-induced apoptosis via the cytosolic $NADH/NAD^+$ redox state. Apoptosis 26: 38-51, 2021.
54. Ferrer CM, Lynch TP, Sodi VL, Falcone JN, Schwab LP, Peacock DL, Vocadlo DJ, Seagroves TN and Reginato MJ: O-GlcNAcylation regulates cancer metabolism and survival stress signaling via regulation of the HIF-1 pathway. Mol Cell 54: 820-831, 2014.
55. Blum A, Mostow K, Jackett K, Kelty E, Dakpa T, Ryan C and Hagos E: KLF4 regulates metabolic homeostasis in response to stress. Cells 10: 830, 2021.
56. Harris JC, Scully MA and Day ES: Cancer cell membrane-coated nanoparticles for cancer management. Cancers (Basel) 11: 1836, 2019.
57. Liu X, Nie L, Zhang Y, Yan Y, Wang C, Colic M, Olszewski K, Horbath A, Chen X, Lei G, *et al*: Actin cytoskeleton vulnerability to disulfide stress mediates disulfidptosis. Nat Cell Biol 25: 404-414, 2023.